HHS Public Access

Author manuscript

Hear Res. Author manuscript; available in PMC 2018 June 01.

Published in final edited form as:

Hear Res. 2017 June ; 349: 208–222. doi:10.1016/j.heares.2017.03.005.

Tinnitus and Hyperacusis: Contributions of Paraflocculus, Reticular Formation and Stress

Yu-Chen Chen[1,2], **Guang-Di Chen**[2,*], **Ben Auerbach**[2], **Senthilvelan Manoha**[2], **Kelly Radziwon**[2], and **Richard Salvi**[2]

[1]Department of Radiology, Nanjing First Hospital, Nanjing Medical University, 210006 Nanjing, China

[2]Center for Hearing and Deafness, SUNY at Buffalo, Buffalo, NY 14214, USA

Abstract

Tinnitus and hyperacusis are common and potentially serious hearing disorders associated with noise-, age- or drug-induced hearing loss. Accumulating evidence suggests that tinnitus and hyperacusis are linked to excessive neural activity in a distributed brain network that not only includes the central auditory pathway, but also brain regions involved in arousal, emotion, stress and motor control. Here we examine electrophysiological changes in two novel non-auditory areas implicated in tinnitus and hyperacusis: the caudal pontine reticular nucleus (PnC), involved in arousal, and the paraflocculus lobe of the cerebellum (PFL), implicated in head-eye coordination and gating tinnitus and we measure the changes in corticosterone stress hormone levels. Using the salicylate-induced model of tinnitus and hyperacusis, we found that long-latency (>10 ms) sound-evoked response components in both the brain regions were significantly enhanced after salicylate administration, while the short-latency responses were reduced, likely reflecting cochlear hearing loss. These results are consistent with the central gain model of tinnitus and hyperacusis, which proposes that these disorders arise from the amplification of neural activity in central auditory pathway plus other regions linked to arousal, emotion, tinnitus gating and motor control. Finally, we demonstrate that salicylate results in an increase in corticosterone level in a dose-dependent manner consistent with the notion that stress may interact with hearing loss in tinnitus and hyperacusis development. This increased stress response has the potential to have wide-ranging effects on the central nervous system and may therefore contribute to brain-wide changes in neural activity.

Graphical abstract

[*]**Send correspondence to:** Guang-Di Chen, Ph.D., Center for Hearing and Deafness, State University of New York at Buffalo, 137 Cary Hall, 3435 Main Street, Buffalo, NY 14214, USA, Tel: +1-716-829-5298, Fax: +1-716-829-2980; gchen7@buffalo.edu.

Conflict of Interest: The authors declare that they have no conflict of interest.

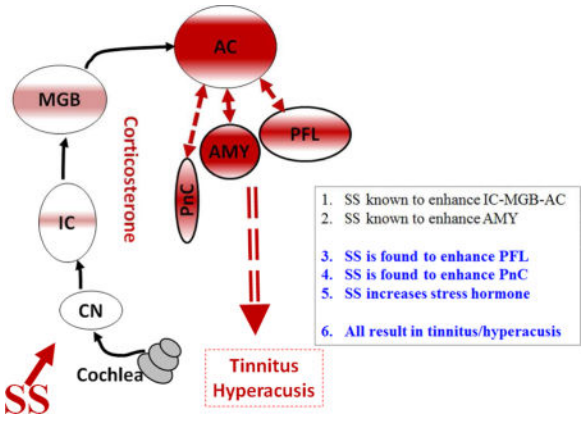

Keywords

Tinnitus; Hyperacusis; Paraflocculus; Reticular Formation; Corticosterone; Salicylate; Stress

Introduction

Military personnel, mostly those in combat, often develop noise-induced hearing loss (NIHL) (Cave et al., 2007; Helfer et al., 2011), a condition exacerbated in some individuals by tinnitus (a phantom buzzing or ringing sensation) and hyperacusis (sounds perceived as intolerably loud or even painful) (Gilles et al., 2012; Henry et al., 2014; Sun, 2011). Recent evidence suggests that tinnitus and hyperacusis arise from maladaptive neuroplastic changes in a distributed neural network that involves portions of the central auditory pathway plus direct and indirect neural connections with other brain regions associated with arousal, stress, anxiety and attention (Auerbach et al., 2014; Baguley et al., 2013; Dornhoffer et al., 2006; Leaver et al., 2016; Lockwood et al., 1999; Moller, 2003). A common feature of intense noise or ototoxic drug exposure is that they reduce the neural output from the cochlea (hypoactivity). To adapt to this altered acoustic input homeostatic mechanisms in the central nervous system “kick in” and increase the gain at successively higher levels of the auditory pathway (Auerbach et al., 2014; Turrigiano, 1999). By the time the neural activity reaches the medial geniculate body (MGB) and auditory cortex (AC) sound-evoked responses are generally larger than normal, a phenomenon referred to as enhanced central gain (Brotherton et al., 2015; Chambers et al., 2016; Chen et al., 2016; Qiu et al., 2000; Salvi et al., 1990). In the case of salicylate-induced hearing loss where there is consistent evidence of tinnitus and hyperacusis, our functional magnetic resonance imaging (fMRI) studies revealed neural hyperactivity in an auditory network consisting of AC, MGB and inferior colliculus (IC) (Figure 1A) plus an emotional center, the amygdala (AMY), that is linked to the AC (Antunes and Moita, 2010; Chen et al., 2015; Newton et al., 2004) (Figure 1). Unexpectedly, salicylate-induced hyperactivity was also observed in the reticular formation (RF), an area of the brain involved in arousal and sleep, and the paraflocculus (PFL), a part of the cerebellum involved in head-eye motor control and which receives some auditory inputs (Azizi and Woodward, 1990; Horikawa and Suga, 1986). When a functional connectivity analysis was performed on our fMRI data, the AC was found to be strongly coupled to both the RF and PFL.

Paraflocculus and Reticular Formation

Although the PFL is best known for its role in coordinating eye and head movements (Nagao, 1992; Rambold et al., 2002), some neurons in this region respond to sound through direct and indirect connections with neurons in the cochlear nucleus (CN), IC and AC (Aitkin and Boyd, 1978; Azizi et al., 1990; Azizi et al., 1985; Azizi et al., 1981; Horikawa et al., 1986; Huang and Liu, 1990; Huang et al., 1982; Kawamura, 1975; Lockwood et al., 1999; Misrahy et al., 1961; Morest et al., 1997; Snider, 1950; Snider, 1948). The cerebellum in turn can influence the auditory system (Rossi et al., 1967; Velluti and Crispino, 1979). Importantly, recent studies suggest that the PFL is involved in gating or regulating tinnitus and hyperacusis (Bauer et al., 2013; Chen et al., 2015). In the case of chronic noise-induced tinnitus, manganese enhanced magnetic resonance imaging (MEMRI) revealed enhanced spontaneous activity in the PFL. Moreover, behavioral evidence of chronic noise-induced tinnitus was abolished by lesioning or inactivating the PFL (Bauer et al., 2013; Brozoski et al., 2007; Brozoski et al., 2013). Collectively, the imaging and behavioral results suggest that the PFL is involved in gating or modulating tinnitus and hyperacusis. In the case of salicylate-induced tinnitus, fMRI revealed enhanced spontaneous activity in the PFL and stronger functional coupling between the PFL and the AC as well (Chen et al., 2015) (Figure 1B). Salicylate also enhances spontaneous activity in the RF and increased the functional coupling between the RF and the AC (Figure 1B). The RF plays an important role in generating the acoustic startle reflex, a strong reflex movement of the head, neck and eyes elicited by brief sound at intensities above ~75 dB SPL. Acoustic signals for eliciting the startle reflex are routed through the cochlear nerve root and the PnC to facial and spinal cord motor neurons that produce abrupt motor responses linked to the acoustic startle reflex (Davis et al., 1982; Lee et al., 1996). Interestingly, high doses of sodium salicylate (SS) greatly enhance the amplitude of the acoustic startle reflex (Lu et al., 2011). Recent research suggests that the preceding effects could be mediated locally or modulated by descending effects from the IC, AC or AMY (Bowen et al., 2003; Chen et al., 2012; Du et al., 2011; Yeomans et al., 2006).

Altogether, the composite results reviewed above suggest that the perceptual features or salience of SS-induced tinnitus may arise from enhanced spontaneous activity, decreased inhibition, increased excitation and/or increased functional connectivity in a distributed network involving the AC, AMY, RF and PFL. While both MEMRI and fMRI imaging techniques revealed enhanced activity in the PFL and RF in animals with noise-induced and salicylate-induced tinnitus, these imaging techniques cannot identify the exact nature of the electrophysiological changes such as distinguishing between hyperactivities resulting from decreased inhibition or increased excitation. To provide relevant physiological measurements relevant to these imaging studies, we carried out electrophysiological recordings from the PFL and the PnC in rats before and after treatment with a high-dose of salicylate where hyperactivity was observed by fMRI measurement. The rationale for recording from the PnC is based on the fact that giant neurons in this region play a critical role in generating the acoustic startle reflex (Lingenhohl and Friauf, 1992), which has been shown to become hyperactive after high-dose SS (Lu et al., 2011). While hearing loss may be a prerequisite for developing tinnitus and hyperacusis, it may be necessary but not a sufficient condition for developing these disorders because many individuals with hearing

loss do not develop tinnitus or hyperacusis. A number of studies suggest that stress combined with auditory impairment may interact synergistically to promote the development of tinnitus and/or hyperacusis or alternatively to contribute to the severity of these conditions such as becoming more bothersome (Alpini and Cesarani, 2006; Hasson et al., 2011; Kim et al., 2012; Mazurek et al., 2012). Stress increases corticosterone stress hormones and enhances sound-evoked activity in the auditory cortex (Ma et al., 2015). High doses of salicylate also increased c-fos expression (a transcription factor that regulates gene expression) in areas of the brain associated with stress (Wallhausser-Franke, 1997; Wallhausser-Franke et al., 2003). Salicylate also induces cochlear hearing loss and enhances sound evoked activity in the central auditory system; the combination of these effects may help to explain why salicylate reliably induces tinnitus and hyperacusis. To determine if salicylate-induced tinnitus and hyperacusis are correlated and linked to stress, we treated rats with different doses of SS and measured serum corticosterone stress hormone levels at various times following the salicylate treatment.

Methods

Experiment 1: Electrophysiology of PFL and PnC

Subjects—MaleSprague–Dawley rats (Charles River Laboratories Inc.) 2–3 months of age were used for the electrophysiological studies. Rats were given free access to food and water and maintained at 22 °C on a 12 light/dark cycle.

Sodium salicylate—SS (Sigma-Aldrich) was dissolved in sterile saline (50 mg/ml). Rats were treated with 250 mg/kg (S.C.) during the electrophysiological experiment.

Electrophysiology—Most of the experimental methods have been described in detail in earlier publications (Chen et al., 2016; Chen et al., 2013). Briefly, rats were deeply anesthetized with ketamine (50 mg/kg, I.M.) and xylazine (6 mg/kg, I.M.) and placed in a stereotaxic apparatus with two ear bars. The dorsal surface of the skull was exposed and cleaned; a small screw was inserted into the right parietal bone and a head bar holder attached to the head screw using dental cement. Then the right ear bar was removed to allow the right ear to be acoustically stimulated free-field using a loudspeaker (FT28D, Fostex) located 10 cm in front of the right ear. Since our imaging data suggested that the PFL responds to sounds presented to the contralateral ear, an opening was made on the lateral part of occipital bone covering the left PFL and a 16-channel linear silicon microelectrode (A-1×16–10mm 100–177, NeuroNexus Technologies) was inserted into the PFL (Lockwood et al., 1999). Recording electrodes were also inserted into the left PnC using stereotaxic coordinates (Watson and Paxinos, 2004). Tone bursts and broadband noise bursts (50 ms duration, 1 ms rise/fall time, cosine^2-gating) were generated using TDT hardware (TDT RX6-2, ~100 kHz sampling rate) and presented with an interstimulus interval (ISI) of 500 ms unless stated otherwise. The sound levels of the tones and broadband noise at the location of the right ear was calibrated by using a sound level meter (Larson Davis, model 2221) with a ¼″ microphone (Larson Davis, model 2520). The biological signals picked by the electrode were sampled with a resolution of 40.96 μs using a RA16PA preamplifier and RX5 base station (Tucker-Davis Technologies System-3, Alachua, FL) using custom-written

data acquisition and analysis software (MATLAB R2007b, MathWorks) as previously described (Chen et al., 2012; Chen et al., 2014; Stolzberg et al., 2011). The neural signals were filtered (300–3500 Hz) for collection of spikes from multiunit clusters (MUC), the threshold for detecting spikes was set manually. To record the local field potentials (LFP) from each electrode, the neural signals were low-pass filtered (2–300 Hz) and down-sampled online with a resolution of 1.64 ms. LFPs were evoked with noise-bursts (see above, 100 presentations) and tone-bursts (see above, 1.0, 1.5, 2.3, 3.5, 5.3, 8.0, 12.1, 18.3, 27.7, and 42.0 kHz, 50 presentations) presented in pseudo random order from 0 to 100 dB in 10 dB steps.

Experiment 2: Salicylate and Corticosterone

Subjects—Thirty-two male Sprague-Dawley rats (Charles River Laboratories Inc.) 2–3 months of age and weighing between 250 and 350 g were used in experiment 2. Twenty-four rats were used for the salicylate dose-response study and eight rats were used for the salicylate time-course study. Prior to starting the experiment, all animals were handled by the same experimenter for 5 days to acclimate the animals to handling and the environment and minimize baseline stress levels.

SS Treatments—SS (Sigma-Aldrich) was dissolved in saline (50 mg/ml) and administered by intraperitoneal injection. The 24 rats used for the salicylate dose-response study were divided into four groups (n = 6/group) and treated with 0, 50, 150 or 250 mg/kg of SS. The injections were given 8:00 AM. Afterwards, the rats were left undisturbed for 2 h in their home cages in a room in which they had been previously acclimated. At 10:00 AM the animals were euthanized with CO_2, decapitated and trunk blood collected from each animal. This whole process was completed within 3 minutes after removing the rat from its cage. The serum was isolated from trunk blood for analysis of blood salicylate concentrations using the Trinder method and blood corticosterone levels measured with a commercial ELISA kit. The eight rats used for the within-subject, time-course study were injected with 250 mg/kg salicylate or saline at 8:00 AM. Saphenous vein blood sampling occurred at 2, 24, and 48 h post-injection. In order to obtain a baseline estimate of corticosterone, a blood sample was collected from each animal 2 h after saline injection (0 mg/kg salicylate). Baseline blood samples were obtained 48 h prior to salicylate injections. All blood samples were collected at 10:00 AM to avoid variations due to circadian rhythms (Atkinson and Waddell, 1997). Following injections, the animals were left undisturbed in their home cages as above. Blood samples were obtained from the saphenous vein after shaving off the overlying hair. Prior to sampling, the area was wiped with 70% ethanol and allowed to dry. Then a thin layer of petroleum jelly was applied to the shaved area. The animal was held with pressure applied to the saphenous vein downstream of the shaved area. Then a small puncture was made in the saphenous vein with an 18 gauge needle after which a small droplet of blood formed on the petroleum jelly on the shaved skin; the blood droplets was drawn into a microcentrifuge tube.

Corticosterone and Salicylate Quantification—Within 30 minutes following collection, blood samples were centrifuged at 1000 RCF for 20 minutes and serum collected for analysis. The isolated serum was stored at − 20 °C. A competitive corticosterone enzyme

immunoassay (EIA) kit was used to quantify the corticosterone concentration in serum samples per the manufacturer's instructions (Enzo Life Sciences, Corticosterone EIA Kit, ADI-900-097). A modified Trinder Method (Trinder, 1954) was used to quantify serum salicylate levels. The Trinder reagent (4% Ferric Nitrate (Sigma Chemical Co.) in 0.12 N HCl) was mixed with the serum samples at a ratio of 1 part serum to 5 parts Trinder reagent. The samples were centrifuged at 1000 RCF for 3 minutes and the absorbance values were read at a wavelength of 540 nm. The average salicylate values from the control group (no salicylate) were subtracted from the salicylate values obtained from animals injected with salicylate (250, 150, 50 mg/kg) to obtain the final salicylate concentration for each sample.

Statistical analysis—GraphPad Prism (version 5) was used for the statistical analyses and graphical presentation as described below.

All the procedures used in this project were approved by the Institutional Animal Care and Use Committee (IACUC-HER05080Y) at the University at Buffalo and carried out in accordance with NIH guidelines.

Results

Experiment 1: Electrophysiological Changes

PFL LFPs—In normal controls, noise bursts evoked distinct LFPs in ~60% (86/144) of the recording sites in the PFL. This percentage increased to ~70% (102/144) after SS treatment. Figure 2A presents the mean LFP in response to 100 dB noise bursts; the data were obtained from the 102 recording sites that generated a response after SS treatment. The mean LFP consists of 4 positive peaks at ~10, 50, 100, and 200 ms following stimulus onset, the positive peaks hereafter referred to as P10, P50, P100, and P200 respectively. Nearly all of the individual LFP waveforms contained P50 and P10, but P100 and P200 were only present in ~80–90% of the samples. After SS treatment, the sound-evoked LFPs were enhanced mainly during the late phase of the response. Figure 2B presents mean LFPs of 52 of the 102 recordings which showed large SS-induced increases in the 15–100 ms interval after stimulation onset, but not in the early period (<15 ms) or late period (>150 ms). Figure 2C presents mean LFPs of the remaining 50 recordings. The pre-SS LFPs were slightly larger than in Figure 1B and the post-SS amplitude enhancement was not as pronounced as in Figure 2B. In these cases, the SS-enhancement was most pronounced in the negative peak at 15–30 ms (Figure 2C, star), but the early response at P10 was reduced (Figure 2C, arrow).

Because the SS-induced changes in LFP amplitude occurred mainly during the first 100 ms, the root mean squares (RMS) of the LFP was computed from 0–100 ms and plotted as a function of intensity. Figure 3A presents the mean (+/−SEM) LFP amplitude as a function of intensity pre-and 2 h post-SS for all 102 LFP recordings. There was a clear overall increase in PFL amplitude 2 h post-SS at stimulation levels higher than 70 dB SPL. A two way, repeated measures ANOVA revealed a significant effect of SS treatment ($F = 6.482$, 1, 1000, DF, $p=0.0124$) and Bonferroni post-tests revealed significant differences at 80, 90 and 100 dB SPL ($p<0.05$). Figure 3B shows the LFP input/output function from the 52 recordings where SS caused a pronounced effect (See Figure 2B). The pre-SS input/output function increased slowly with intensity and the maximum pre-SS response was roughly 8.8 μV at

100 dB SPL. At 2 h post-SS, the response amplitude at 100 dB SPL was nearly 20 μV, roughly twice as large as the pre-SS value. A two way, repeated measures ANOVA revealed a significant pre-post difference ($F=23.57$, 1, 1020 DF, $p<0.0001$) and Bonferroni post-tests revealed significant post-SS amplitude increases from 70 dB to 100 dB SPL ($p<0.01$). Figure 3C shows the mean (+/− SEM) input/output function from the 50 recordings where SS had little effect on LFP from the PFL. In this subpopulation, SS has no effect on the LFP input/output function. Figure 3D shows the LFP amplitude measured at 100 dB SPL across pre- and post-recording times from the 52 recordings where SS had an effect. LFP amplitudes remained stable during the 2 h pre-treatment and immediately after the SS-injection (0 h). LFP amplitude increased from 1 to 2 h, doubling from its baseline amplitude and then decreased between 2 and 4 h post-SS. A one way, repeated measure ANOVA showed a significant change in LFP amplitudes across time ($F=27.68$, 6 and 325 DF, $p<0.0001$). A Newman-Keuls Multiple Comparison Test showed that LFP amplitude Post-1 h ($p<0.01$), Post-2 h ($p<0.001$), Post-3 h ($p<0.001$) and Post-4 h ($p<0.001$) were significantly greater than Pre-1 h amplitudes.

PFL Multiunit Firing Patterns—From the 144 recordings, approximately 20% (n=29) produced an increase in firing rate to noise burst or tone burst. Most of the MUC (22/29) responded to both noise bursts and tone bursts; however, three responded exclusively to noise while four responded only to tones. Figure 4 shows the peristimulus time histograms (PSTHs) of a MUC to 50 ms noise-bursts presented at 100 dB SPL pre- and 1 to 4 h post-SS. The peak firing rate in the PSTH occurred 25–30 ms after noise burst onset. SS yielded a robust increase in firing rate that reached a maximum at 2–3 h post-SS (Figure 4D–E). Ten MUC produced PSTH similar to those shown in Figure 4. The PSTHs from these 10 MUC were averaged to form a mean PSTH pre- and 2 h post-SS (Figure 5A, pre = blue line, red = 2 h post SS). The PSTH 2 h post-SS showed a clear increase in firing rate during the noise bursts (Figure 5A). A two way ANOVA was performed on the first 50 ms of mean PSTH showing a significant increase in firing rate 2 h post-SS compared to pre-SS ($F = 45.54$, 1, 450 DF, $p<0.0001$). Eight MUC did not show a clear increase in discharge rate in response to 100 dB noise-burst pre-SS; however, after SS treatment their firing rates increased. The PSTHs from these weakly activated MUC were averaged together pre- and 2 h post-SS (Figure 5B, pre = blue, red = 2 h post-SS). After SS treatment, the mean PSTHs showed a large increase in firing rate, the mean firing rate gradually increased reaching a peak around 70 ms that was followed by a gradual decline toward baseline around 100 ms. A two way ANOVA performed on the first 100 ms of mean PSTHs revealed a significant increase in firing rate 2 h post-SS compared to pre-SS ($F=140.2$, 1, 700 df, $p<0.0001$). Figure 5C presents the mean PSTH of 7 MUC to 100 dB noise bursts. The pre-SS PSTH contained a short-latency (~3 ms) (pre = blue line) onset response followed by later peaks in the PSTH. The short latency onset response was vanished 2 h post-SS, whereas the later responses remained largely unchanged. The mean discharge rate in the 100 ms time window did not change significantly post- SS.

The 10 MUC that responded to 100 dB SPL noise bursts with a long latency (Figure 6A, bottom row) responded most robustly to low and mid-frequency tone bursts. To illustrate this overall trend, a mean PSTH was computed for tone bursts ranging from 1 to 27.7 kHz.

Figure 6A shows the mean PSTHs obtained with 100 dB SPL tone bursts (50 ms duration) pre- (blue line) and 2 h post-SS (red line). The pre-treatment PSTHs showed clear increases in firing rate at 1.0, 2.3, 3.5, 5.3, and 8.0 kHz and much weaker responses from 12.1–27.7 kHz (Figure 6A, all rows except bottom). The maximum firing rate in the PSTHs occurred 10–15 ms after stimulus onset. At 2 h post-SS, there was a clear increase in firing rate at all frequencies, even at the three highest frequencies where baseline responses were weak or absent. The post-SS responses were significantly greater than the pre-SS responses at all frequencies (Two-way, repeated measures ANOVA performed on the first 50 ms of each mean PSTH,1, 450 DF, $p<0.0001$; F-levels presented in the figure). Mean tone burst PSTHs were computed for another 16 MUC that responded weakly or not at all to noise bursts (Figure 6B, bottom panel). Most of these MUC only responded to low-frequency tone bursts (1.0–3.5 kHz) before SS-treatment and their discharge rates at these frequencies increased significantly 2 h post-SS (Figure 6B, all row except bottom, Two-way, repeated measure ANOVA performed on the first 50 ms of each mean PSTH, 1, 750 DF, $p<0.0001$, F values shown in figure). SS not only increased the maximum discharge rate but also prolonged the duration of the tone burst evoked response (e.g., 1 kHz, Figure 6B).

PnC Multiunit Firing Patterns—MUC in the PnC contralateral to the stimulated ear responded most robustly to noise bursts (50 ms) with a short onset latency of ~4 ms followed by a gradual decrease in firing rate as illustrated by the PSTH in figure 7A. When the intensity of the noise burst increased, the discharge rate of the MUC increased monotonically (Figure 7B). PnC MUCs responded to tone bursts in a frequency dependent manner as illustrated by the matrix of PSTH in figure 7C. At 100 dB SPL, robust PSTH responses occurred over a broad frequency range, but at 70 dB, the largest PSTH responses were present within 1–1.5 kHz and smaller PSTH responses were still present at 5.3 and 12.1 kHz (red arrows). The general impression gleaned from Figure 7C is that PnC MUC have relatively high thresholds and are broadly tuned. This interpretation is reinforced by the frequency-threshold tuning curves from 8 MUC shown in Figure 7D. Most PnC MUC only responded to tone bursts at 60 dB SPL or higher and the frequency-threshold turning curves of all 8 MUC were fairly broad.

Figure 8A presents mean discharge rate-intensity function to 50 ms noise-burst recorded from 8 PnC MUC in one rat. Firing rates in 50 ms time window remained consistent 1 to 3 h prior to SS treatment. After SS treatment, the response threshold increased ~30 dB; however, the firing rate evoked by suprathreshold stimuli (>70 dB) increased dramatically. Figure 8B shows the discharge rates at 50 dB (near threshold) and 100 dB (suprathreshold) plotted as a function of time pre- and post-SS. The discharge rates at 50 dB SPL decreased between 0 and 2 h post-SS due to the increase in threshold. In contrast, the firing rates at 100 dB SPL gradually increased from 0 to 3 h post-SS. The firing rate 3 h post-SS was roughly 70% higher than pre-treatment value, but then declined somewhat at 4 h post-SS. Figure 8C shows the mean discharge rate-intensity function for noise bursts obtained from 41 PnC MUC measured in four rats. The function was shifted to the right roughly 20 dB at low intensities, but firing rates at suprathreshold levels were slightly higher 2 hours poss-SS.

The preceding results were obtained with an interstimulus interval or ISI of 500 ms. However, because neurons in the reticular formation habituate to acoustic stimuli presented

at high repetition rates, the firing patterns of PnC neurons were evaluated with different ISI (0.25 to 10 s) before and after SS treatment (Lingenhohl and Friauf, 1994). The firing rates and firing patterns of PnC MUC were highly sensitive to ISI and to SS. In general, firing rates were much greater at long versus short ISI. In addition, the effects of SS on PSTH firing profiles were time dependent and ISI dependent as illustrated by the mean PSTH from 65 PnC MUC obtained with 100 dB noise bursts presented with an ISI of 0.25 s (Figure 9A) and 10 s (Figure 9B). SS enhanced the late component (> 15 ms) of PSTH profile at both short (Figure 9A) and long ISIs (Figure 9B). In addition, SS increased the latency and reduced the amplitude of the large onset peak of the PSTH.

To quantify the changes in discharge rate due to ISI and SS, mean discharge rates were computed in four time windows of the mean PSTH (3–6, 7–10, 11–20 and 21–54 ms) and plotted as a function of ISI pre- and post-SS. Firing rates in all four time windows increased monotonically as ISI increased from 0.25 s to 10 s. SS caused a decrease in firing rate in the 3–6 ms early response window at all ISI; this decrease is likely due to the SS-induced increase in latency of the PSTH peak (see Figure 9A–B). There was a significant effect of ISI (two way repeated measure ANOVA, $F = 4.84, 3, 38$ DF, $p < 0.01$), but no significant effect of SS or interaction between SS and ISI (Figure 9C). SS caused an increase in firing rate in the 7–10 ms time window (Figure 9D). There was a significant effect of ISI (two way repeated measure ANOVA, $F = 60.17, 3, 38$ DF, $p< 0.0001$) and ISI by treatment interaction ($F = 5.530, 3, 38$ DF, $p < 0.01$), but the effect of SS was not significant. SS caused a large increase in discharge rate in the 11–20 ms response window (Figure 9E). The effect of ISI (two way repeated measure ANOVA, $F = 117.5, 3, 98$ DF, $p < 0.0001$), SS treatment ($F = 11.51, 1, 98$ DF, $p <0.001$) and ISI by treatment interaction ($F =22.32, 3, 98$ DF, $p < 0.0001$) were significant. The largest SS-induced increase in firing rate occurred in the 51–54 ms window. The effect of ISI (two way repeated measure ANOVA, $F = 610.3, 3, 66$ DF, $p < 0.0001$), SS treatment ($F= 329.7, 1, 66$ DF, $p < 0.0001$) and ISI by treatment interaction ($F = 7.2, 3, 66$ DF, $p < 0.0001$) were significant. As noted above (Figure 6), PnC MUC tended to respond more robustly to low frequencies than to high frequencies pre- and post-SS. Figure 10 presents mean PSTHs of 54 MUC to low-frequency tones <10 kHz (A) and high-frequency tones >10 kHz (B) at 100 dB SPL. Interestingly, the SS-enhancement was observed for the responses to the low frequencies but not for the responses to the high frequencies.

Experiment 2: SS-Induced Corticosterone Increases

Dose-Response—To determine if SS induced a stress response we measured corticosterone in serum after administration of SS. Two h after intraperitoneal injection with 0, 50, 150 or 250 mg/kg of SS, mean (+/− SEM, n=4) serum SS levels were 0, 194, 462 and 638 μg/ml respectively (Figure 11A, right ordinate). Serum salicylate concentrations were significantly greater than saline control levels for the 50, 150, and 250 mg/kg doses of salicylate (Newman-Keuls post hoc analysis, $p < 0.05$). The mean plasma corticosterone values were 40.9, 32.8, 351.0 and 772.5 ng/ml in the groups treated with 0, 50, 150 and 250 mg/kg of SS (Figure 11A, left ordinate). There was a significant effect of SS dose ($F = 27.88, 3, 19$ DF, $p < 0.001$). Serum corticosterone concentrations in the 50 mg/kg group were similar to the control group whereas serum corticosterone concentrations in the 250

mg/kg group were significantly greater than the control group (Newman-Keuls post-hoc analysis, $p < 0.05$, $). Although serum corticosterone concentrations in the 150 mg/kg group were higher than controls, the difference did not reach statistical significance.

Time-Course—SS-induced ototoxicity, tinnitus and hyperacusis typically disappear a day or two days post-treatment. To determine how long it would take for serum SS and corticosterone to recover, serial blood samples were first collected from each rat 2 h after saline treatment and then again 2, 24 and 48 h after treatment with 250 mg/kg salicylate. The mean (n = 8, +/− SEM) salicylate values at 2, 24, and 48 h post-SS were 579.3, 155.7, and 7.00 μg SS/ml serum respectively versus 0.2 μg for the saline control (Figure 11B, right ordinate). The mean (n =8, +/− SEM) serum SS concentrations at 2 h and 24 h post-SS were significantly greater than the saline control (one-way ANOVA, treatment effect, $p<0.0001$, $F= 68, 3, 22$ DF, Tukey's Multiple comparison, $p<0.05$). The SS injections resulted in a large increase in serum corticosterone 2 h post-SS that decreased at later time points (Figure 11B, left ordinate). The average corticosterone concentration in the saline group was 17.44 ng/ml serum vs. 334.1, 49.8 and 26.9 ng/ml serum in the SS group at 2, 24 and 48 h post-treatment (Figure 11B); only the corticosterone level at 2 h post-SS was significantly higher than the saline control (one-way ANOVA, treatment effect $p < 0.0001$, $F= 15.83, 3, 28$ DF, Tukey's multiple comparison, $p<0.05$).

Salicylate-Corticosterone Correlation—Figure 11C shows the relationship between the corticosterone levels and the serum salicylate concentrations for all the three salicylate doses at 2 h post-treatment. A Richard's five-parameter dose-response sigmoidal function was fit to the serum salicylate-corticosterone response function (R^2: 0.7649, 18 DF). The maximum corticosterone concentration found following saline injections was 114.2 ng/ml of serum. The serum SS concentrations lower than ~400 μg/ml serum evoked no corticosterone response while the higher SS concentrations produced a large increase in corticosterone. The salicylate serum concentration (Log EC50) needed to evoke a half-maximum corticosterone response was 543.4 mg/ml (99% confidence interval: 427.2 – 659.5).

Discussion

Previous studies have shown that SS causes hyperactivity in selected regions of the central auditory pathway and the AMY (Figure 1) (Chambers et al., 2016; Chen et al., 2013; Lu et al., 2011; Norena et al., 2010; Qiu et al., 2000; Stolzberg et al., 2011; Syka and Rybalko, 2000; Zhang et al., 2011). Our more recent fMRI studies identified two additional areas outside the classical auditory pathway where SS induced hyperactivity, named the PFL and RF (Chen et al., 2015). To confirm and characterize the electrophysiological changes that occur in these non-auditory regions, we recorded LFP and MUC firing patterns from the PFL and PnC before and after SS treatment and measured the changes in serum corticosterone to evaluate the potential contribution of this stress hormone. The three new findings of the current study are that: (1) high-dose SS causes a subset of neurons in the PFL and PnC to become hyperactive to suprathreshold acoustic stimuli, (2) the firing rate and SS-induced hyperactivity in the PnC increases significantly with increasing ISI and (3) high doses of SS (≥ 150 mg/kg) known to induce tinnitus and hyperacusis cause a large increase in corticosterone stress hormone levels. Our results suggest that SS-induced hyperactivity

observed in selected parts of the central nervous system may be linked to the upregulation of circulating corticosterone stress hormone or the receptors to which it binds (Ma et al., 2015).

Auditory PFL

Several parts of the cerebellum respond to auditory stimulation including the PFL (Altman et al., 1976; Azizi et al., 1990; Azizi et al., 1985; Azizi et al., 1981; Buser and Franchel, 1960; Huang and Liu, 1985; Huang and Burkard, 1986; Huang and Liu, 1991; Lockwood et al., 1999; Lorenzo et al., 1977; Mihailoff et al., 1981; Misrahy et al., 1961; Petacchi et al., 2005; Snider and Stowell, 1944; Snider et al., 1964; Stowell, 1942; Wolfe, 1972; Woody et al., 1999). Noise bursts evoked distinct LFPs in ~60% (86/144) of our recording sites in the PFL (Figure 2). The latency of the LFPs evoked by 100 dB noise burst presented to the contralateral ear and the onset response of most PSTH MUC were relatively long on the order of 10 ms; these results are consistent with the long latency responses seen in the paraflocculus of the mustache bat (Horikawa et al., 1986). The long-latency PFL-responses may reflect a long signaling pathway through high auditory levels like the AC, which showed SS-enhancing effect, whereas the short-latency PFL-responses (Fig. 5C) may reflect a short signaling pathway through lower levels of the auditory pathway such as IC and even more peripheral parts of the auditory pathway showing no SS-enhancing effect. In addition, the PSTH profiles and the peaks in the LFP waveforms were relatively broad. Taken together, these results suggest that the inputs to the contralateral PFL were relayed to it from one or more higher auditory centers such as the IC or AC (Azizi et al., 1985; Brodal, 1968). Moreover, relatively high intensity noise bursts (>60 dB) were needed to elicit a robust LFP (Figure 3). PFL MUC were most responsive to low frequency tone bursts and their tuning was relatively broad (1–8 kHz, see Figure 6), consistent with results from mustache bat (Horikawa et al., 1986).

LFP amplitudes and MUC discharge rates increased significantly after SS treatment. The nature of the SS-effects was linked to the latency of the response. The early response (<15 ms) was typically reduced whereas the late response was enhanced post-SS (Figure 2C, 5C, 9A and B, 10A). The early PFL-response may reflect direct input from the cochlea and/or cochlear nucleus, regions where the sound-evoked responses are reduced post-SS. The increased responsivity of the late component post-SS could be due to diminished inhibition or increased excitation within the PFL itself or to the AC or IC that relay information to the PFL. It has to be noted that this facilitative effect occurred only in half of the recordings. Because SS induces robust hyperactivity in the AC, it is possible that the ensuing hyperactivity in the PFL is influenced by the AC neuronal activity. However, this interpretation is tempered by the fact that electrical stimulation of the AC and IC produces a mixture of excitatory and inhibitory responses in the PFL (Azizi et al., 1985). In the AC and AMY, SS-treatment caused the frequency receptive fields of low frequency neurons to shift upward toward the mid-frequencies (Chen et al., 2012; Lobarinas, 2006; Stolzberg et al., 2011; Yamamoto et al., 2007). However, there was little evidence of an upward shift in the PFL (Figure 6).

At a systems level, the PFL receives multiple types of sensory information, including inputs from vestibular and auditory centers. The prevailing view is that this information is

integrated and processed in order to fine tune head and eye movements such as those used to direct the head and eyes toward or away from a sound source, such as the echo orientation system in bats (Horikawa et al., 1986). Interestingly, some vestibular schwannoma patients develop gaze-evoked tinnitus, a condition in which deviation of the eyes from straight ahead alters the loudness or pitch of tinnitus (Cacace et al., 1996; Coad et al., 2001; Lockwood et al., 2001; van Gendt et al., 2012). Eye movements have also been shown to modulate tinnitus in non-tumor patients (Simmons et al., 2008). Taken together, these results suggest that the eye-movement circuitry of the PFL may be involved in modulating tinnitus.

One consequence of the SS-induced hyperactivity in the PFL is that it could speed up and/or facilitate such motor activity. Consistent with this view, we have found using an operant-conditioning paradigm that assesses loudness growth, that SS induces a reduction in subjects' reaction times (shorter latency) in response to sounds of moderate to high intensity (Chen et al., 2015). Functional imaging studies have also suggested that the PFL is involved in gating or modulating tinnitus (Brozoski et al., 2007; Chen et al., 2015). This interpretation was supported by behavioral studies showing that tinnitus was suppressed or enhanced by inactivating or activating the PFL (Bauer et al., 2013; Brozoski et al., 2007; Brozoski et al., 2013). Noise-induced spontaneous hyperactivity in the IC, considered a neural correlate of tinnitus, is enhanced by removal of the PFL whereas PFL removal had no effect on spontaneous activity in normal animals (Vogler et al., 2016). If spontaneous hyperactivity in the IC is a neural indicator of tinnitus (Manzoor et al., 2013), then these results suggest that PFL removal would enhance tinnitus, an interpretation at odds with behavioral data showing that PFL inactivation suppresses tinnitus (Bauer et al., 2013).

PnC Hyperactivity

A loud, abrupt and unexpected sound induces the acoustic startle reflex. The acoustic startle circuit consists of cochlear root neurons, neurons in the PnC, and motor neurons. Repetitive sound stimuli induce startle reflexes with long ISI, but not short ISI. This gating effect appeared to result from the PnC response which increases with increase of ISI (see Fig. 9). In addition, only high level sounds above 70 dB SPL induce startle reflexes. This is consistent with the high thresholds (>65–70 dB SPL) observed in our PnC responses (Fig. 7). High doses of SS significantly enhance the amplitude of the acoustic startle reflex (Chen et al., 2014; Du et al., 2011). Since SS greatly reduces the neural output of the cochlea at suprathreshold levels, the mechanisms for enhancing acoustic startle amplitudes must occur beyond the cochlear nerve root either in the PnC or the facial and spinal motor neurons that drive the musculature responsible for the startle reflex (Davis et al., 1982; Lee et al., 1996). Our results show that SS significantly increased the discharge rate of PnC MUC to high-intensity noise bursts (Figure 8A–B), intensities that are typically needed to induce the startle reflex. SS shifted the low-intensity portion of our discharge rate-intensity functions to the right 20–30 dB. This threshold shift is consistent with and likely due to the cochlear hearing loss induced by SS (Chen et al., 2013; Stolzberg et al., 2011). Since we are unaware of any evidence indicating that SS enhances motor neuron output, our results suggest that the SS-induced increase in startle amplitude has its origins in the PnC or hyperactivity from descending inputs to the PnC from the AC, AMY or IC (Chen et al., 2015). This interpretation is consistent with several features of PnC discharge patterns. First, the neural

output of the PnC and the amplitude of the startle reflex continue to increase with ISI extending out tens of seconds or more (Hoffman and Fleshler, 1963; Ison and Hammond, 1971). Second, PnC MUC responded most robustly to tone bursts below 10 kHz (Figure 10) consistent with large startle responses to lower frequency tone bursts (Blaszczyk and Tajchert, 1997). Because SS mainly enhanced the discharge to tone bursts below 10 kHz, one might expect that SS would selectively increase startle amplitude to low (<10 kHz), but not to high frequency tone bursts. The effects of SS on PnC firing patterns were duration dependent. SS mainly enhanced PnC firing during the late portion of the PSTH and this effect was ISI dependent. Based on these results, SS would presumably cause the greatest increase in startle amplitude at long ISI and long duration noise bursts. The effects of SS on startle amplitude would likely be minimal for short duration noise bursts and short ISIs (Figure 9).

Corticosterone Upsurge

Because high doses of SS produced strong c-fos immunolabeling in brain areas associated with stress, anxiety and pain (Wallhausser-Franke, 1997; Wallhausser-Franke et al., 2003), we hypothesized that SS would significantly increase corticosterone levels. Our results are generally consistent with these predictions. High doses of SS sufficient to induce tinnitus (Guitton et al., 2003; Jastreboff et al., 1988; Lobarinas et al., 2004; Ruttiger et al., 2003) caused a large increase in serum corticosterone levels whereas low doses incapable of inducing tinnitus had almost no effect on corticosterone levels. The 250 mg/kg SS dose caused ~18-fold increase in corticosterone over baseline (Figure 11) whereas 150 mg/kg induced ~8 fold increase. The large variability associated with the 150 mg/kg dose of SS may be related to the fact that this dose lies near the threshold for inducing tinnitus (Lobarinas et al., 2004). Twenty-four hours after the cessation of salicylate, corticosterone levels decreased to near control levels consistent with previous behavioral studies showing the disappearance of tinnitus one day after discontinuing SS (Guitton et al., 2003; Lobarinas et al., 2004). Corticosterone levels in response to a stressor normally have a half-life of 25–60 minutes (Haemisch et al., 1999; Vachon and Moreau, 2001); however, our results show that corticosterone levels did not approach baseline levels until 24 h post-treatment. These results indicate that high doses of salicylate can disrupt the hypothalamic-pituitary-adrenal (HPA) system for a prolonged period of time resulting in abnormally high corticosterone levels. Corticosterone is normally bound to carrier proteins and is inactive as it is transported through the circulatory system. Corticosterone binding globulin (CBG), the dominant carrier protein, binds approximately 90% of circulating corticosterone. When corticosterone is released from CBG it can bind to glucocorticoid receptors and exert numerous biological effects (Ekins, 1992). Interestingly, in fluorometric assays, salicylate is used to free corticosterone from CBG (Erkens et al., 1998; Kane, 1979; Shrivastav, 2004). This raises the possibility that high levels of serum SS promotes the release of corticosterone from CBG resulting in a large unbound pool of serum corticosterone consistent with our results (Figure 11A–B). The SS-induced increases in corticosterone may also contribute to sound-induced hyperactivity in the AC, MGB and AMY (Chen et al., 2013; Lu et al., 2011; Yang et al., 2007), the same regions where SS increased c-fos expression (Wallhausser-Franke, 1997). Interestingly, rodent repellent stressors that increase serum corticosterone significantly increased the amplitude of auditory evoked responses (Mazurek et al., 2010). Moreover,

exogenous corticosterone enhances auditory evoked potential amplitudes (Maxwell et al., 2006). Taken together, these results suggest that the hyper or altered activity is due to increases in corticosterone levels.

Acknowledgments

Research supported in part by grants from the National Institutes of Health (R01DC014452, R01DC014693) and ONR (N000141210731). The authors thank Brandon Decker for assistance with collecting and analyzing the serum salicylate and corticosterone data in experiment 2.

References

Aitkin LM, Boyd J. Acoustic input to the lateral pontine nuclei. Hear Res. 1978; 1:67–77. [PubMed: 757232]

Alpini D, Cesarani A. Tinnitus as an alarm bell: stress reaction tinnitus model. ORL J Otorhinolaryngol Relat Spec. 2006; 68:31–6. discussion 36–7. [PubMed: 16514260]

Altman JA, Bechterev NN, Radionova EA, Shmigidina GN, Syka J. Electrical responses of the auditory area of the cerebellar cortex to acoustic stimulation. Exp Brain Res. 1976; 26:285–98. [PubMed: 991958]

Antunes R, Moita MA. Discriminative auditory fear learning requires both tuned and nontuned auditory pathways to the amygdala. J Neurosci. 2010; 30:9782–7. [PubMed: 20660260]

Atkinson HC, Waddell BJ. Circadian variation in basal plasma corticosterone and adrenocorticotropin in the rat: sexual dimorphism and changes across the estrous cycle. Endocrinology. 1997; 138:3842–8. [PubMed: 9275073]

Auerbach BD, Rodrigues PV, Salvi RJ. Central gain control in tinnitus and hyperacusis. Front Neurol. 2014; 5:206. [PubMed: 25386157]

Azizi SA, Woodward DJ. Interactions of visual and auditory mossy fiber inputs in the paraflocculus of the rat: a gating action of multimodal inputs. Brain Res. 1990; 533:255–62. [PubMed: 2289142]

Azizi SA, Burne RA, Woodward DJ. The auditory corticopontocerebellar projection in the rat: inputs to the paraflocculus and midvermis. An anatomical and physiological study. Exp Brain Res. 1985; 59:36–49. [PubMed: 4018197]

Azizi SA, Mihailoff GA, Burne RA, Woodward DJ. The pontocerebellar system in the rat: an HRP study. I. Posterior vermis. J Comp Neurol. 1981; 197:543–8. [PubMed: 7229127]

Baguley D, McFerran D, Hall D. Tinnitus. Lancet. 2013; 382:1600–7. [PubMed: 23827090]

Bauer CA, Kurt W, Sybert LT, Brozoski TJ. The cerebellum as a novel tinnitus generator. Hear Res. 2013; 295:130–9. [PubMed: 23418634]

Blaszczyk JW, Tajchert K. Effect of acoustic stimulus characteristics on the startle response in hooded rats. Acta Neurobiol Exp (Wars). 1997; 57:315–21. [PubMed: 9519548]

Bowen GP, Lin D, Taylor MK, Ison JR. Auditory cortex lesions in the rat impair both temporal acuity and noise increment thresholds, revealing a common neural substrate. Cereb Cortex. 2003; 13:815–22. [PubMed: 12853367]

Brodal P. The corticopontine projection in the cat. I. Demonstration of a somatotopically organized projection from the primary sensorimotor cortex. Exp Brain Res. 1968; 5:210–34. [PubMed: 5721752]

Brotherton H, Plack CJ, Maslin M, Schaette R, Munro KJ. Pump up the volume: could excessive neural gain explain tinnitus and hyperacusis? Audiol Neurootol. 2015; 20:273–82. [PubMed: 26139435]

Brozoski TJ, Ciobanu L, Bauer CA. Central neural activity in rats with tinnitus evaluated with manganese-enhanced magnetic resonance imaging (MEMRI). Hear Res. 2007; 228:168–79. [PubMed: 17382501]

Brozoski TJ, Wisner KW, Odintsov B, Bauer CA. Local NMDA receptor blockade attenuates chronic tinnitus and associated brain activity in an animal model. PLoS One. 2013; 8:e77674. [PubMed: 24282480]

Buser P, Franchel H. Existence of a focus of acoustic sensory projection at the level of the ansiform lobe of the cerebellum in the cat. C R Hebd Seances Acad Sci. 1960; 251:791–3.

Cacace, AT., Lovely, TJ., Parnes, SM., Winter, DF., McFarland, DJ. Gaze-evoked tinnitus following unilateral peripheral auditory deafferentation: A case for anamolous cross modality plasticity. In: Salvi, RJ.Henderson, D.Fiorino, F., Colletti, V., editors. Auditory System Plasticity and Regeneration. Thieme Medical Publishers; New York: 1996. p. 1354-1358.

Cave KM, Cornish EM, Chandler DW. Blast injury of the ear: clinical update from the global war on terror. Mil Med. 2007; 172:726–30. [PubMed: 17691685]

Chambers AR, Resnik J, Yuan Y, Whitton JP, Edge AS, Liberman MC, Polley DB. Central Gain Restores Auditory Processing following Near-Complete Cochlear Denervation. Neuron. 2016; 89:867–79. [PubMed: 26833137]

Chen GD, Manohar S, Salvi R. Amygdala hyperactivity and tonotopic shift after salicylate exposure. Brain Res. 2012; 1485:63–76. [PubMed: 22464181]

Chen GD, Sheppard A, Salvi R. Noise trauma induced plastic changes in brain regions outside the classical auditory pathway. Neuroscience. 2016; 315:228–45. [PubMed: 26701290]

Chen GD, Radziwon KE, Kashanian N, Manohar S, Salvi R. Salicylate-induced auditory perceptual disorders and plastic changes in nonclassical auditory centers in rats. Neural Plast. 2014; 2014:658741. [PubMed: 24891959]

Chen GD, Stolzberg D, Lobarinas E, Sun W, Ding D, Salvi R. Salicylate-induced cochlear impairments, cortical hyperactivity and re-tuning, and tinnitus. Hear Res. 2013; 295:100–13. [PubMed: 23201030]

Chen YC, Li X, Liu L, Wang J, Lu CQ, Yang M, Jiao Y, Zang FC, Radziwon K, Chen GD, Sun W, Krishnan Muthaiah VP, Salvi R, Teng GJ. Tinnitus and hyperacusis involve hyperactivity and enhanced connectivity in auditory-limbic-arousal-cerebellar network. Elife. 2015; 4:e06576. [PubMed: 25962854]

Coad ML, Lockwood A, Salvi R, Burkard R. Characteristics of patients with gaze-evoked tinnitus. Otol Neurotol. 2001; 22:650–4. [PubMed: 11568674]

Davis M, Gendelman DS, Tischler MD, Gendelman PM. A primary acoustic startle circuit: lesion and stimulation studies. J Neurosci. 1982; 2:791–805. [PubMed: 7086484]

Dornhoffer J, Danner C, Mennemeier M, Blake D, Garcia-Rill E. Arousal and attention deficits in patients with tinnitus. Int Tinnitus J. 2006; 12:9–16. [PubMed: 17147035]

Du Y, Wu X, Li L. Differentially organized top-down modulation of prepulse inhibition of startle. J Neurosci. 2011; 31:13644–53. [PubMed: 21940455]

Ekins R. The free hormone hypothesis and measurement of free hormones. Clin Chem. 1992; 38:1289–93. [PubMed: 1307685]

Erkens JH, Dieleman SJ, Dressendorfer RA, Strasburger CJ. A time-resolved fluoroimmunoassay for cortisol in unextracted bovine plasma or serum with optimized procedures to eliminate steroid binding protein interference and to minimize non-specific streptavidin-europium binding. J Steroid Biochem Mol Biol. 1998; 67:153–61. [PubMed: 9877216]

Gilles A, De Ridder D, Van Hal G, Wouters K, Kleine Punte A, Van de Heyning P. Prevalence of leisure noise-induced tinnitus and the attitude toward noise in university students. Otol Neurotol. 2012; 33:899–906. [PubMed: 22722146]

Guitton MJ, Caston J, Ruel J, Johnson RM, Pujol R, Puel JL. Salicylate induces tinnitus through activation of cochlear NMDA receptors. J Neurosci. 2003; 23:3944–52. [PubMed: 12736364]

Haemisch A, Guerra G, Furkert J. Adaptation of corticosterone-but not beta-endorphin-secretion to repeated blood sampling in rats. Lab Anim. 1999; 33:185–91. [PubMed: 10780823]

Hasson D, Theorell T, Wallen MB, Leineweber C, Canlon B. Stress and prevalence of hearing problems in the Swedish working population. BMC Public Health. 2011; 11:130. [PubMed: 21345187]

Helfer TM, Jordan NN, Lee RB, Pietrusiak P, Cave K, Schairer K. Noise-induced hearing injury and comorbidities among postdeployment U.S. Army soldiers: April 2003-June 2009. Am J Audiol. 2011; 20:33–41. [PubMed: 21474555]

Henry JA, Roberts LE, Caspary DM, Theodoroff SM, Salvi RJ. Underlying mechanisms of tinnitus: review and clinical implications. J Am Acad Audiol. 2014; 25:5–22. quiz 126. [PubMed: 24622858]

Hoffman HS, Fleshler M. Startle Reaction: Modification by Background Acoustic Stimulation. Science. 1963; 141:928–30. [PubMed: 14043340]

Horikawa J, Suga N. Biosonar signals and cerebellar auditory neurons of the mustached bat. J Neurophysiol. 1986; 55:1247–67. [PubMed: 3734857]

Huang C, Liu G. Organization of the auditory area in the posterior cerebellar vermis of the cat. Exp Brain Res. 1990; 81:377–83. [PubMed: 2397763]

Huang CM, Liu G. Electrophysiological mapping of the auditory areas in the cerebellum of the cat. Brain Res. 1985; 335:121–9. [PubMed: 4005535]

Huang CM, Burkard R. Frequency sensitivities of auditory neurons in the cerebellum of the cat. Brain Res. 1986; 371:101–8. [PubMed: 3708338]

Huang CM, Liu GL. Auditory responses in the posterior vermis of the cat: the buried cerebellar cortex. Brain Res. 1991; 553:201–5. [PubMed: 1933280]

Huang CM, Liu G, Huang R. Projections from the cochlear nucleus to the cerebellum. Brain Res. 1982; 244:1–8. [PubMed: 7116161]

Ison JR, Hammond GR. Modification of the startle reflex in the rat by changes in the auditory and visual environments. J Comp Physiol Psychol. 1971; 75:435–52. [PubMed: 5091224]

Jastreboff PJ, Brennan JF, Coleman JK, Sasaki CT. Phantom auditory sensation in rats: an animal model for tinnitus. Behav Neurosci. 1988; 102:811–22. [PubMed: 3214530]

Kane JW. Use of sodium salicylate as a blocking agent for cortisol-binding-globulin in a radioimmunoassay for cortisol on unextracted plasma. Ann Clin Biochem. 1979; 16:209–12. [PubMed: 533227]

Kawamura K. The pontine projection from the inferior colliculus in the cat. An experimental anatomical study. Brain Res. 1975; 95:309–22. [PubMed: 1156878]

Kim YH, Jung HJ, Kang SI, Park KT, Choi JS, Oh SH, Chang SO. Tinnitus in children: association with stress and trait anxiety. Laryngoscope. 2012; 122:2279–84. [PubMed: 22886845]

Leaver AM, Seydell-Greenwald A, Rauschecker JP. Auditory-limbic interactions in chronic tinnitus: Challenges for neuroimaging research. Hear Res. 2016; 334:49–57. [PubMed: 26299843]

Lee Y, Lopez DE, Meloni EG, Davis M. A primary acoustic startle pathway: obligatory role of cochlear root neurons and the nucleus reticularis pontis caudalis. J Neurosci. 1996; 16:3775–89. [PubMed: 8642420]

Lingenhohl K, Friauf E. Giant neurons in the caudal pontine reticular formation receive short latency acoustic input: an intracellular recording and HRP-study in the rat. J Comp Neurol. 1992; 325:473–92. [PubMed: 1281843]

Lingenhohl K, Friauf E. Giant neurons in the rat reticular formation: a sensorimotor interface in the elementary acoustic startle circuit? J Neurosci. 1994; 14:1176–94. [PubMed: 8120618]

Lobarinas, E. Effects of carboplatin-induced inner hair cell loss on auditory perception in chinchilla. SUNY University at Buffalo; Buffalo: 2006.

Lobarinas E, Sun W, Cushing R, Salvi R. A novel behavioral paradigm for assessing tinnitus using schedule-induced polydipsia avoidance conditioning (SIP-AC). Hear Res. 2004; 190:109–14. [PubMed: 15051133]

Lockwood AH, Salvi RJ, Coad ML, Arnold SA, Wack DS, Murphy BW, Burkard RF. The functional anatomy of the normal human auditory system: responses to 0.5 and 4.0 kHz tones at varied intensities. Cereb Cortex. 1999; 9:65–76. [PubMed: 10022496]

Lockwood AH, Wack DS, Burkard RF, Coad ML, Reyes SA, Arnold SA, Salvi RJ. The functional anatomy of gaze-evoked tinnitus and sustained lateral gaze. Neurology. 2001; 56:472–80. [PubMed: 11222790]

Lorenzo D, Velluti JC, Crispino L, Velluti R. Cerebellar sensory functions: rat auditory evoked potentials. Exp Neurol. 1977; 55:629–36. [PubMed: 858339]

Lu J, Lobarinas E, Deng A, Goodey R, Stolzberg D, Salvi RJ, Sun W. GABAergic neural activity involved in salicylate-induced auditory cortex gain enhancement. Neuroscience. 2011; 189:187–98. [PubMed: 21664433]

Ma L, Zhang J, Yang P, Wang E, Qin L. Acute restraint stress alters sound-evoked neural responses in the rat auditory cortex. Neuroscience. 2015; 290:608–20. [PubMed: 25668592]

Manzoor NF, Gao Y, Licari F, Kaltenbach JA. Comparison and contrast of noise-induced hyperactivity in the dorsal cochlear nucleus and inferior colliculus. Hear Res. 2013; 295:114–23. [PubMed: 22521905]

Maxwell CR, Ehrlichman RS, Liang Y, Gettes DR, Evans DL, Kanes SJ, Abel T, Karp J, Siegel SJ. Corticosterone modulates auditory gating in mouse. Neuropsychopharmacology. 2006; 31:897–903. [PubMed: 16123740]

Mazurek B, Haupt H, Olze H, Szczepek AJ. Stress and tinnitus-from bedside to bench and back. Front Syst Neurosci. 2012; 6:47. [PubMed: 22701404]

Mazurek B, Haupt H, Joachim R, Klapp BF, Stover T, Szczepek AJ. Stress induces transient auditory hypersensitivity in rats. Hear Res. 2010; 259:55–63. [PubMed: 19840840]

Mihailoff GA, Burne RA, Azizi SA, Norell G, Woodward DJ. The pontocerebellar system in the rat: an HRP study. II. Hemispheral components. J Comp Neurol. 1981; 197:559–77. [PubMed: 7229128]

Misrahy GA, Spradley JF, Beran AV, Garwood VP. Acoustic cerebellar pathways in cats. J Neurophysiol. 1961; 24:159–66. [PubMed: 13771300]

Moller AR. Pathophysiology of tinnitus. Otolaryngol Clin North Am. 2003; 36:249–66. v–vi. [PubMed: 12856295]

Morest DK, Kim J, Bohne BA. Neuronal and transneuronal degeneration of auditory axons in the brainstem after cochlear lesions in the chinchilla: cochleotopic and non-cochleotopic patterns. Hear Res. 1997; 103:151–68. [PubMed: 9007582]

Nagao S. Different roles of flocculus and ventral paraflocculus for oculomotor control in the primate. Neuroreport. 1992; 3:13–6. [PubMed: 1611029]

Newton JR, Ellsworth C, Miyakawa T, Tonegawa S, Sur M. Acceleration of visually cued conditioned fear through the auditory pathway. Nat Neurosci. 2004; 7:968–73. [PubMed: 15322551]

Norena AJ, Moffat G, Blanc JL, Pezard L, Cazals Y. Neural changes in the auditory cortex of awake guinea pigs after two tinnitus inducers: salicylate and acoustic trauma. Neuroscience. 2010; 166:1194–209. [PubMed: 20096752]

Petacchi A, Laird AR, Fox PT, Bower JM. Cerebellum and auditory function: an ALE meta-analysis of functional neuroimaging studies. Hum Brain Mapp. 2005; 25:118–28. [PubMed: 15846816]

Qiu C, Salvi R, Ding D, Burkard R. Inner hair cell loss leads to enhanced response amplitudes in auditory cortex of unanesthetized chinchillas: evidence for increased system gain. Hear Res. 2000; 139:153–71. [PubMed: 10601720]

Rambold H, Churchland A, Selig Y, Jasmin L, Lisberger SG. Partial ablations of the flocculus and ventral paraflocculus in monkeys cause linked deficits in smooth pursuit eye movements and adaptive modification of the VOR. J Neurophysiol. 2002; 87:912–24. [PubMed: 11826056]

Rossi G, Cortesina G, Robecchi MG. Cerebellifugal fibres to the cochlear nuclei and superior olivary complex. Acta Otolaryngol. 1967; 63:166–71. [PubMed: 4166312]

Ruttiger L, Ciuffani J, Zenner HP, Knipper M. A behavioral paradigm to judge acute sodium salicylate-induced sound experience in rats: a new approach for an animal model on tinnitus. Hear Res. 2003; 180:39–50. [PubMed: 12782351]

Salvi RJ, Saunders SS, Gratton MA, Arehole S, Powers N. Enhanced evoked response amplitudes in the inferior colliculus of the chinchilla following acoustic trauma. Hear Res. 1990; 50:245–57. [PubMed: 2076976]

Shrivastav TG. Incorporation of different bridge length linkers in enzyme and its use in the preparation of enzyme conjugates for immunoassay. J Immunoassay Immunochem. 2004; 25:215–25. [PubMed: 15461384]

Simmons R, Dambra C, Lobarinas E, Stocking C, Salvi R. Head, Neck and Eye Movements that Modulate Tinnitus. Sem Hear. 2008; 29:361–370.

Snider RS. Recent contributions to the anatomy and physiology of the cerebellum. Arch Neurol Psychiatry. 1950; 64:196–219.

Snider RS, Stowell A. Receiving areas of tactile, auditory and visual systems in the cerebellum. J Neurophysiol. 1944; 1:331–357.

Snider RS, Sato K, Mizuno S. Cerebellar Influences on Evoked Cerebral Responses. J Neurol Sci. 1964; 1:325–39. [PubMed: 14192575]

Snider RS, Eldred E. Cerebral projections to the tactile, auditory and visual areas in the cerebellum. Anat Rec. 1948; 100:82.

Stolzberg D, Chen GD, Allman BL, Salvi RJ. Salicylate-induced peripheral auditory changes and tonotopic reorganization of auditory cortex. Neuroscience. 2011; 180:157–64. [PubMed: 21310217]

Stowell A, Snider RS. Projection of an auditory pathway to the cerebellum of a cat. Anat Rec. 1942; 82:491.

Sun, W., Allman, B., Jayaram, A., Gibson, B. Noise Exposure Induced Hyperacusis Behavior. Association for Research in Otolaryngology; Baltimore, MD: 2011. p. 152

Syka J, Rybalko N. Threshold shifts and enhancement of cortical evoked responses after noise exposure in rats. Hear Res. 2000; 139:59–68. [PubMed: 10601713]

Trinder P. Rapid determination of salicylate in biological fluids. Biochem J. 1954; 57:301–3. [PubMed: 13172184]

Turrigiano GG. Homeostatic plasticity in neuronal networks: the more things change, the more they stay the same. Trends Neurosci. 1999; 22:221–7. [PubMed: 10322495]

Vachon P, Moreau JP. Serum corticosterone and blood glucose in rats after two jugular vein blood sampling methods: comparison of the stress response. Contemporary Topics in Laboratory Animal Science. 2001; 40:22–4.

van Gendt MJ, Boyen K, de Kleine E, Langers DR, van Dijk P. The relation between perception and brain activity in gaze-evoked tinnitus. J Neurosci. 2012; 32:17528–39. [PubMed: 23223277]

Velluti R, Crispino L. Cerebellar actions on cochlear microphonics and on auditory nerve action potential. Brain Res Bull. 1979; 4:621–4. [PubMed: 487218]

Vogler DP, Robertson D, Mulders WH. Influence of the paraflocculus on normal and abnormal spontaneous firing rates in the inferior colliculus. Hear Res. 2016; 333:1–7. [PubMed: 26724754]

Wallhausser-Franke E. Salicylate evokes c-fos expression in the brain stem: implications for tinnitus. Neuroreport. 1997; 8:725–8. [PubMed: 9106755]

Wallhausser-Franke E, Mahlke C, Oliva R, Braun S, Wenz G, Langner G. Expression of c-fos in auditory and non-auditory brain regions of the gerbil after manipulations that induce tinnitus. Exp Brain Res. 2003; 153:649–54. [PubMed: 14508632]

Watson, C., Paxinos, G. The rat brain in stereotaxic coordinates 5th Edition. Elsevier; Academic Press; 2004.

Wolfe JW. Responses of the cerebellar auditory area to pure tone stimuli. Exp Neurol. 1972; 36:295–309. [PubMed: 5053356]

Woody CD, Nahvi A, Palermo G, Wan J, Wang XF, Gruen E. Differences in responses to 70 dB clicks of cerebellar units with simple versus complex spike activity: (i) in medial and lateral ansiform lobes and flocculus; and (ii) before and after conditioning blink conditioned responses with clicks as conditioned stimuli. Neuroscience. 1999; 90:1227–41. [PubMed: 10338293]

Yamamoto E, Takashi T, Morinaka Y, Lin S, Kitano H, Matsuoka M, Ashikari M. Interaction of two recessive genes, hbd2 and hbd3, induces hybrid breakdown in rice. Theor Appl Genet. 2007; 115:187–94. [PubMed: 17487470]

Yang G, Lobarinas E, Zhang L, Turner J, Stolzberg D, Salvi R, Sun W. Salicylate induced tinnitus: behavioral measures and neural activity in auditory cortex of awake rats. Hear Res. 2007; 226:244–53. [PubMed: 16904853]

Yeomans JS, Lee J, Yeomans MH, Steidl S, Li L. Midbrain pathways for prepulse inhibition and startle activation in rat. Neuroscience. 2006; 142:921–9. [PubMed: 16996220]

Zhang X, Yang P, Cao Y, Qin L, Sato Y. Salicylate induced neural changes in the primary auditory cortex of awake cats. Neuroscience. 2011; 172:232–45. [PubMed: 21044658]

Highlights

- Salicylate enhanced auditory response of the cerebellar paraflocculus
- Salicylate enhanced auditory response of the reticular formation
- While the late response component was enhanced the early response was reduced
- Salicylate enhanced serum corticosterone level
- The physiological changes and the stress hormone increase may be involved in tinnitus and hyperacusis

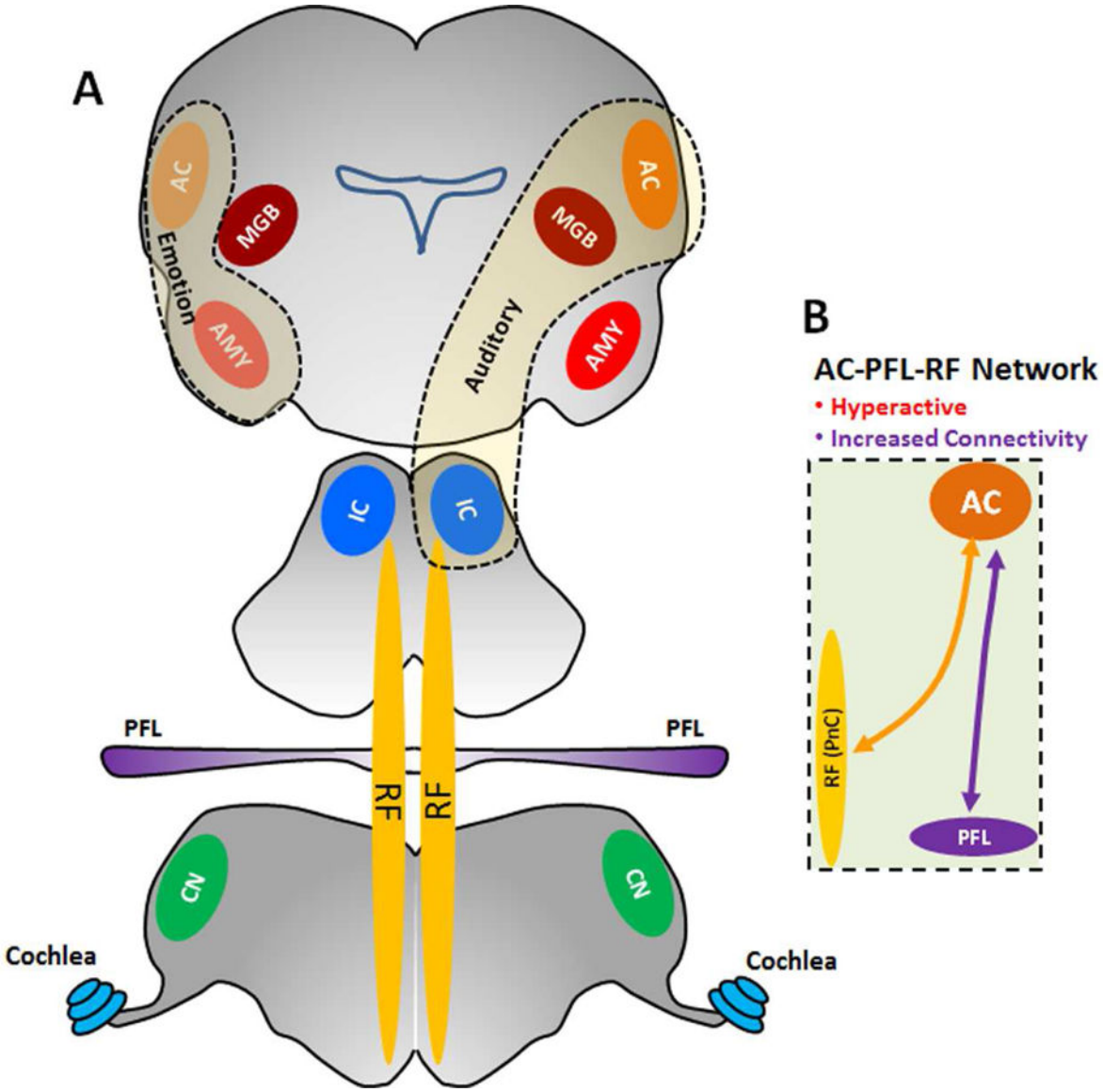

Figure 1.

Model of Tinnitus-Hyperacusis network: (A) High-dose SS induces hyperactivity and increases functional connectivity in an auditory network consisting of AC, MGB and IC (thin dashed line) and emotional network linking the amygdala (AMY) with the AC (thick dashed line). The hyperactivity and enhanced functional connectivity are also occurred in the PFL and RF, areas outside the classical auditory pathway but connected to the AC. (B) SS increases the functional coupling between the AC and the two regions outside the classical auditory pathway, the PFL and RF (PnC).

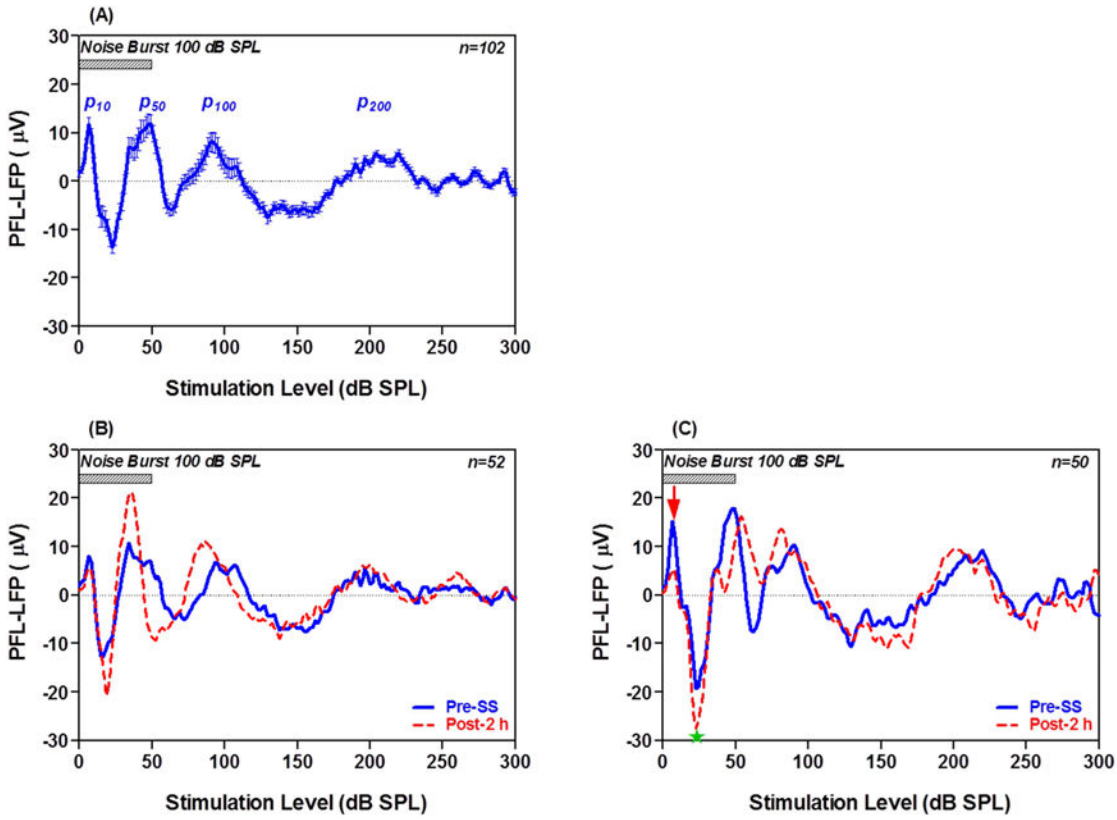

Figure 2.

LFP from PFL evoked by noise bursts pre- and post-SS. (A) Mean (+/− SEM) LFP from 102 recordings before SS treatment; note four positive peaks at 10, 50, 100, and 200 ms after onset of the noise burst (50 ms, 100 dB SPL). (B) Mean LFP from 52 of the 102 recordings with relatively small pre-SS responses (blue) which were enhanced 2 h post-SS (red). (C) Mean LFP of 50 of 102 recordings with relatively large pre-SS responses (blue). SS suppressed the early onset peak at ~10 ms (down red arrow), but enhanced the negative peak (green star) at ~20 ms.

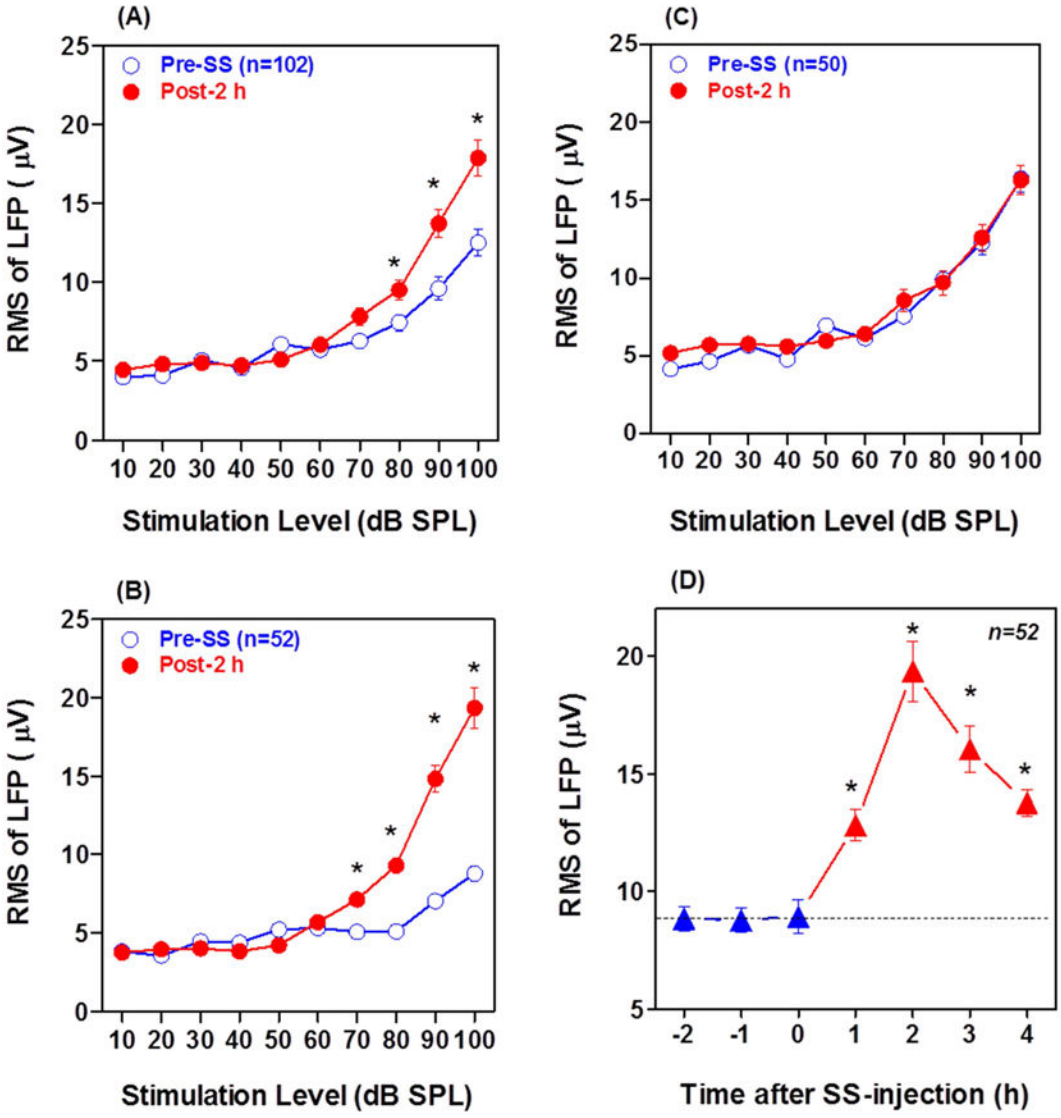

Figure 3.

Pre- and Post-SS LFP amplitude-intensity functions from PFL. RMS of LFP computed from 0–100 ms. (A) Mean (+/− SEM) of all 102 PFL recordings; note significant (*) LFP enhancement from 80–100 dB SPL 2 h post-SS. (B) Mean (+/− SEM) LFP input/output function from 52 of the 102 recordings with small LFPs pre-SS; note significant (*) LFP amplitude enhancement from 70–100 dB SPL 2 h post-SS. (C): Mean (+/− SEM) LFP input/output function from 50 of the 102 recordings with large LFPs pre-SS. LFP input/output function largely unchanged 2 h post-SS. (D) Mean (+/− SEM) LFP amplitude at 100 dB SPL pre-SS (−2, −1 h), immediately after SS treatment (0 h) and 1–4 h post-SS. Note significant (*) increases in LFP amplitude 1–4 h post-SS.

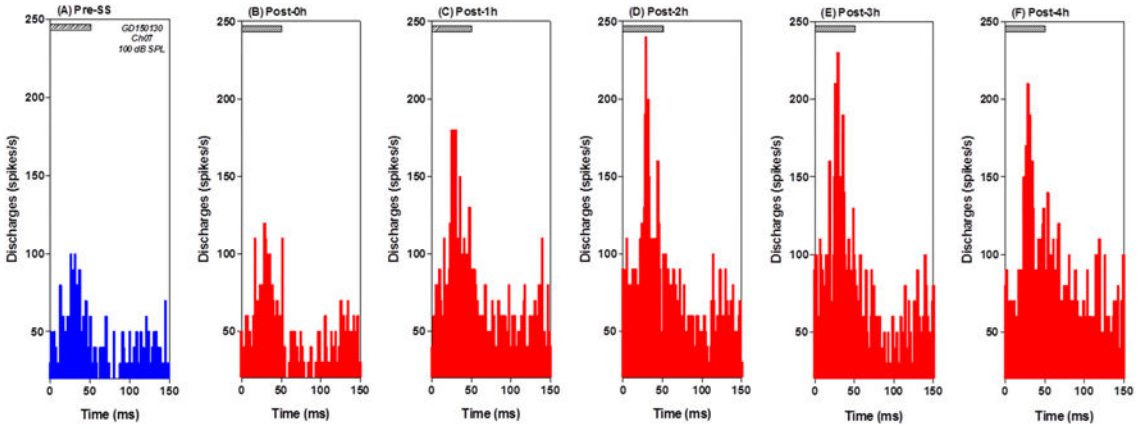

Figure 4.

MUC in PFL show increased firing rates to noise bursts. PSTH from a MUC in the PFL showed strong response to noise bursts (100 dB SPL, 50 ms). (A) PSTHs pre-SS (blue) and (B–F) 0–4 h post-SS (red). Note large increase in firing rate post-SS.

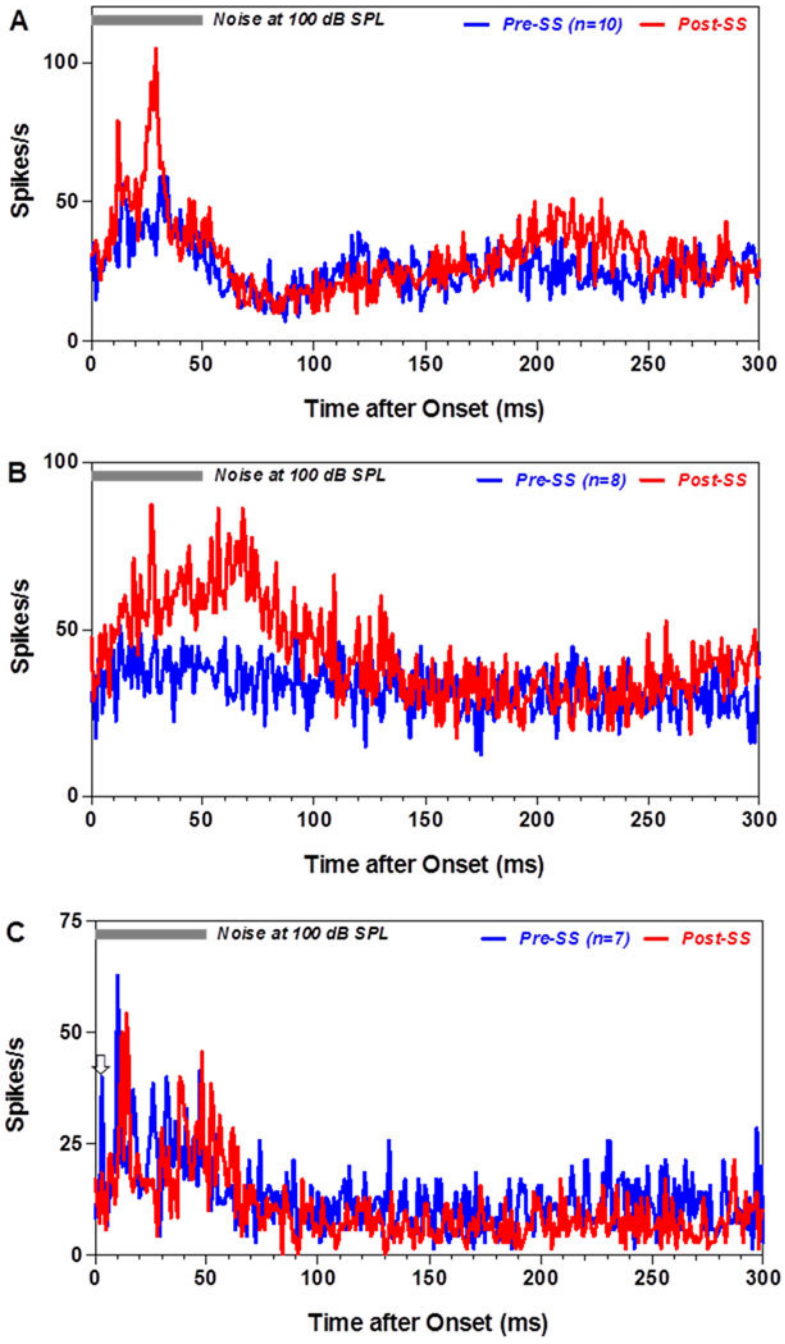

Figure 5.

Effects of SS on discharges of neurons in the PFL to noise bursts. Grand mean PSTHs to 100 dB noise bursts (50 ms) pre- (blue line) and 2 h post-SS (red). (A) Mean PSTHs from 10 MUC in PFL that produced strong response pre- and post-SS. Discharge rate during first 100 ms of PSTH increased significantly post-SS. (B) Mean PSTH from 8 MUC that responded weakly to noise bursts pre-SS. Note large increase in firing rate and broad PSTH 2 h post-SS. (C) Mean PSTHs from 7 MUC with a short-latency (~3 ms) peak in the PSTH pre-SS.

Short-latency, onset response disappeared 2 h post-SS and firing rate was largely unaffected by SS.

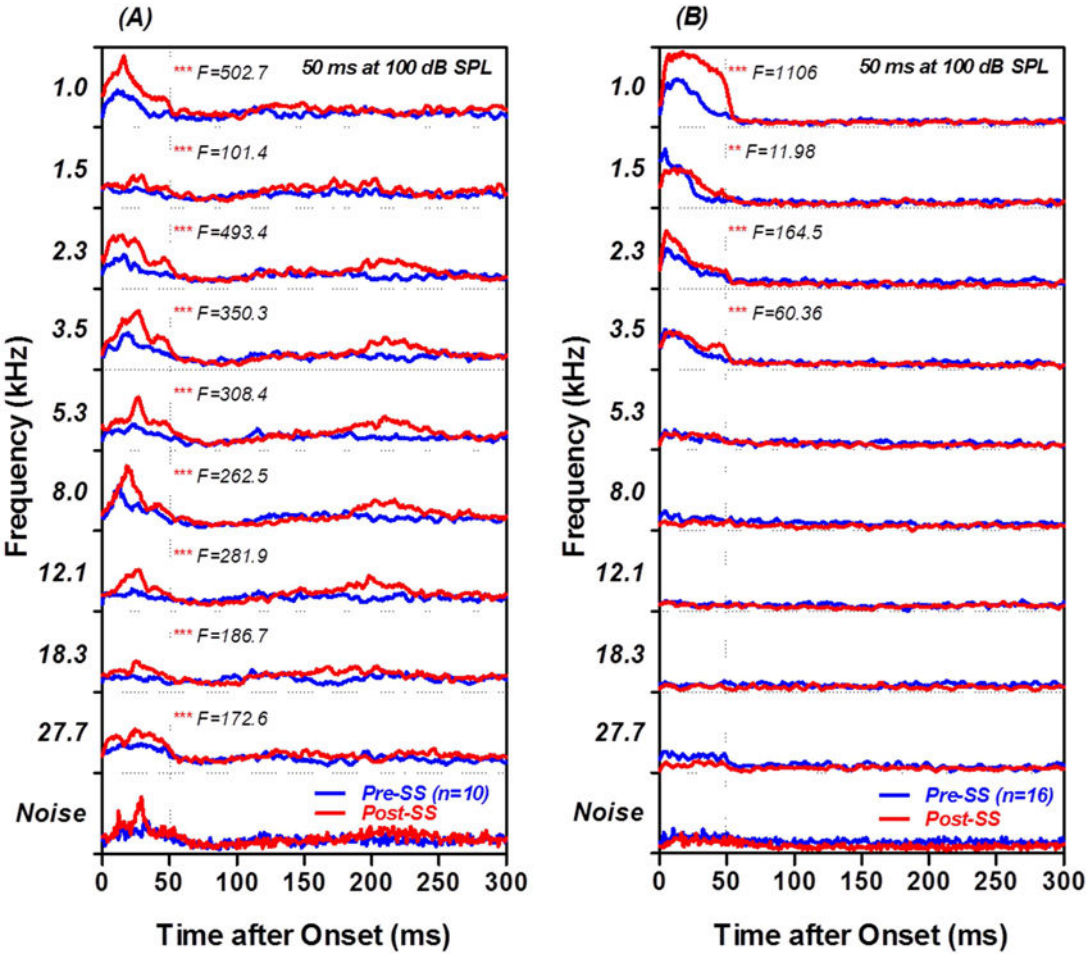

Figure 6.

Tone evoked PSTHs from PFL MUC. (A) Mean PSTHs evoked by 100 dB, 50 ms tone bursts (top 9 rows) from the 10 MUC that responded to noise-burst with long latency (bottom row). Tone bursts from 1–8 kHz evoked distinct PSTH responses pre-SS (blue line); the peak response in the PSTH occurred 15–20 ms after stimulus onset. PSTH response amplitudes were significantly larger 2 h post-SS than before treatment (F values shown in each panel). (B) Mean tone burst evoked PSTH from 16 MUC that responded weakly or not at all to noise bursts. Tone bursts mainly evoked responses from 1–3.5 kHz prior to the SS treatment. PSTH response amplitudes in the 1–3.5 kHz range increased significantly 2 h post-SS (F values shown in figure). ** $p<0.01$, *** $p<0.001$.

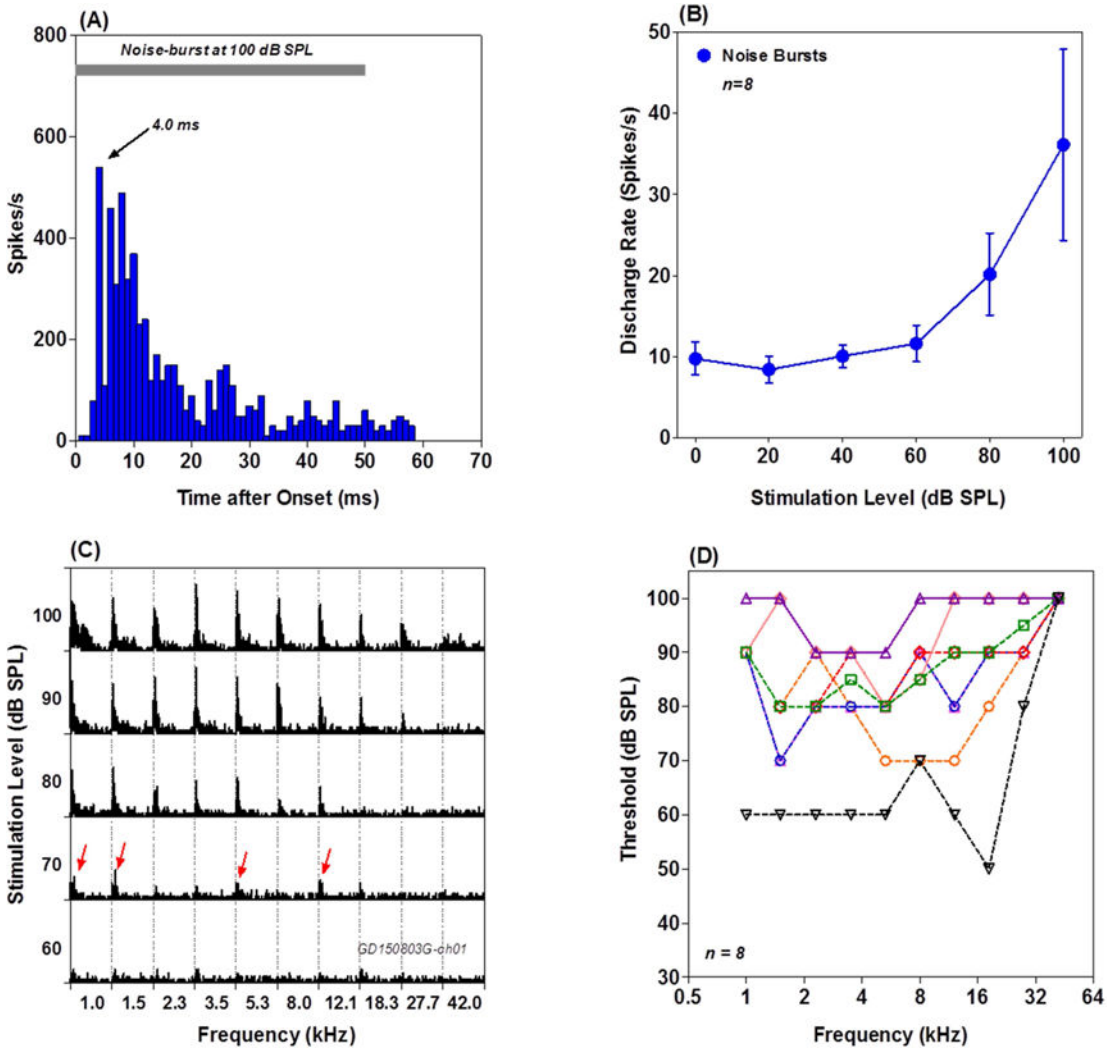

Figure 7.

Response properties of PnC MUC. (A) Representative PSTH from a PnC MUC stimulated with 100 dB noise burst. Note short latency (~ 4 ms) onset response. (B) Mean (n=8, +/− SEM) discharge rate-intensity function of 8 PnC MUC. (C) Frequency-intensity matrix of PSTH obtained with 50 ms tone bursts. Sounds at 70 dB SPL or higher evoked PSTH responses. At 70 dB SPL, responses occurred over a broad frequency range (red arrows). (D) Frequency receptive field of 8 PnC MUC; note broad tuning and high intensities needed to elicit responses.

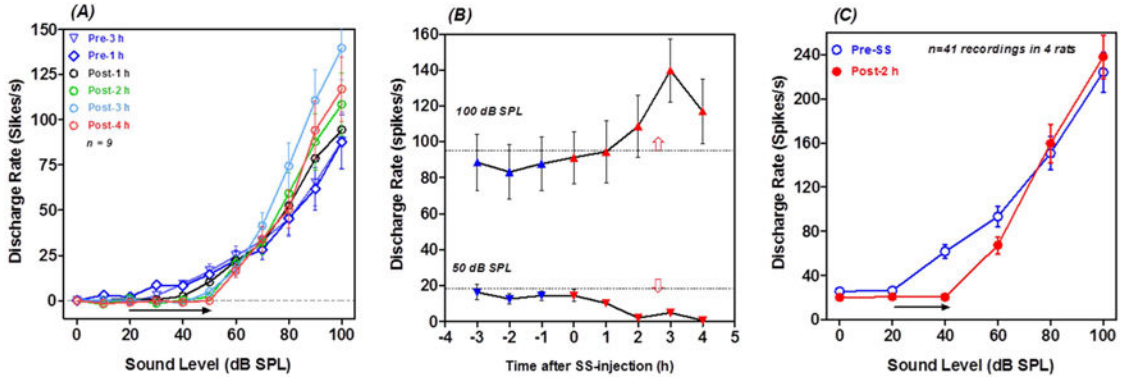

Figure 8.

SS enhances firing rate of PnC MUC. (A) Noise burst, discharge rate-intensity functions from 9 PnC MUC recorded from one rat. Measurements shown for 1 and 3 h pre-SS and 1, 2, 3 and 4 h post-SS. SS increased threshold ~30 dB (horizontal arrow). Note large increase in suprathreshold (>70 dB SPL) firing rates particularly at 3 and 4 h post-SS. (B) Discharge rate at 50 dB and 100 dB SPL plotted as a function of time from the 9 MUC in panel A. Blue symbols show pre-SS and red symbols show post-SS data. Note decrease in firing rate at 50 dB SPL and increase in firing rate at 100 dB SPL during the post-SS period. (C) Mean (n=41 MUC from 4 rats, +/− SEM) discharge rate intensity function for noise bursts from all PnC MUC. Note threshold increase of ~20 dB and slight increase in firing rate at suprathreshold intensities.

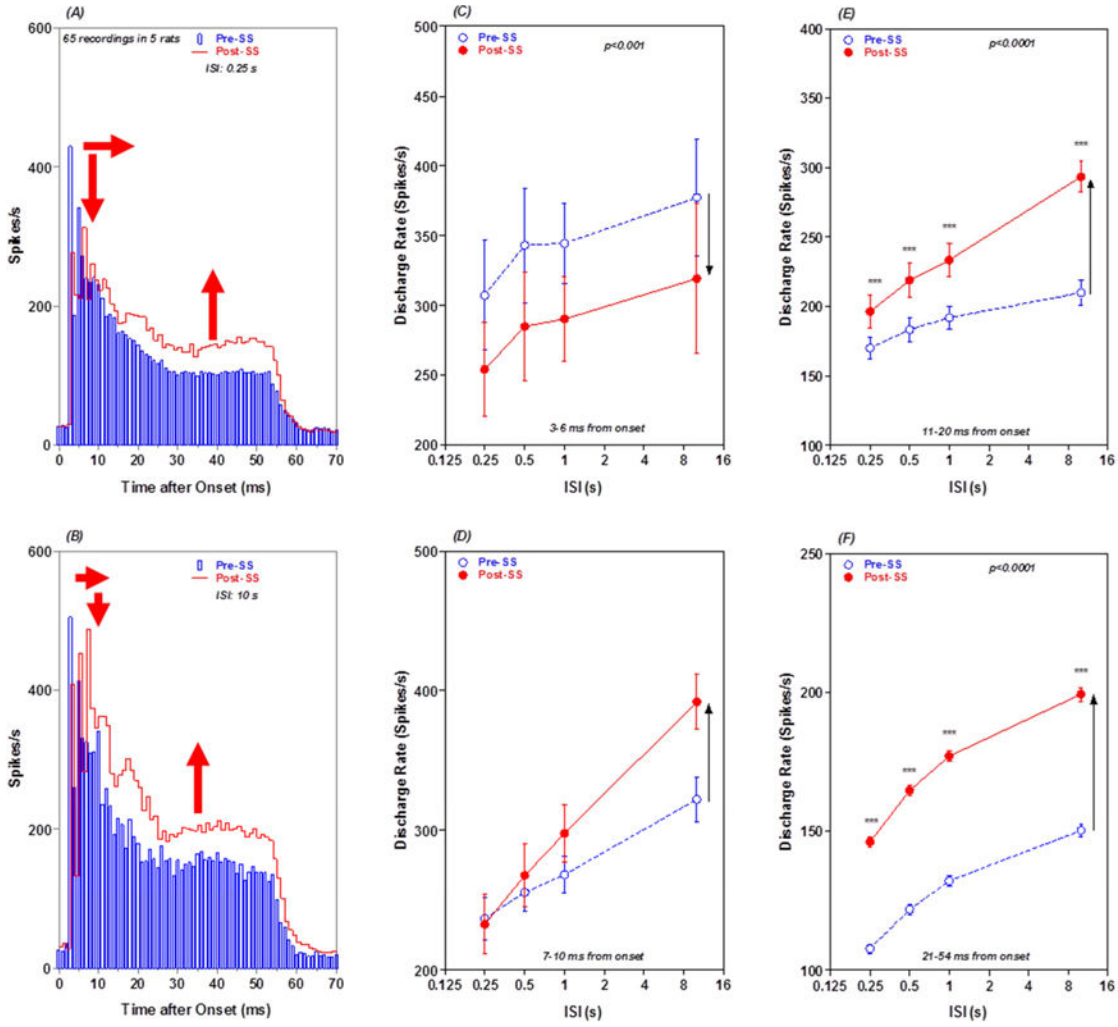

Figure 9.

ISI and SS alter PnC PSTH profiles and discharge rate: (A) Mean PSTH from 65 PnC MUC in response to 100 dB noise bursts presented with an ISI of 0.25 s. Mean PSTH shown pre-SS (blue) and 2 h post-SS (red). Peak of PSTH reduced (down red arrow), latency of PSTH peak prolonged (horizontal red arrow) and late response of PST enhanced (red up arrow) 2 h post SS. (B) Same as panel A except that data collected with ISI of 10 s. Peak of PSTH reduced slightly, latency of PSTH peak increased and late response of PSTH greatly enhanced. (C) Mean (+/−SEM) discharge rates in 3–6 ms (early response) segment of the mean PSTH pre-SS (blue) and 2 h post-SS (red) as a function of ISI. SS caused a large decrease in firing rate at all ISIs (down arrow). (D) Mean (+/−SEM) discharge rates in 7–10 ms segment of the mean PSTH pre-SS (blue) and 2 h post-SS (red) as a function of ISI. SS increased firing rates at ISIs between 0.5 and 10 s (up arrow). SS-induced increases in firing rate increased with increasing ISI. (E) Mean (+/−SEM) discharge rates in 11–20 ms segment of the mean PSTH pre-SS (blue) and 2 h post-SS (red) as a function of ISI. SS increased firing rates at all ISIs. SS-induced increases in firing rate increased with increasing ISI (up arrow). (F) Mean (+/−SEM) discharge rates in 21–54 ms (late response) segment of the

mean PSTH pre-SS (blue) and 2 h post-SS (red) as a function of ISI. SS caused a large increase in firing rates at all ISIs (up arrow).

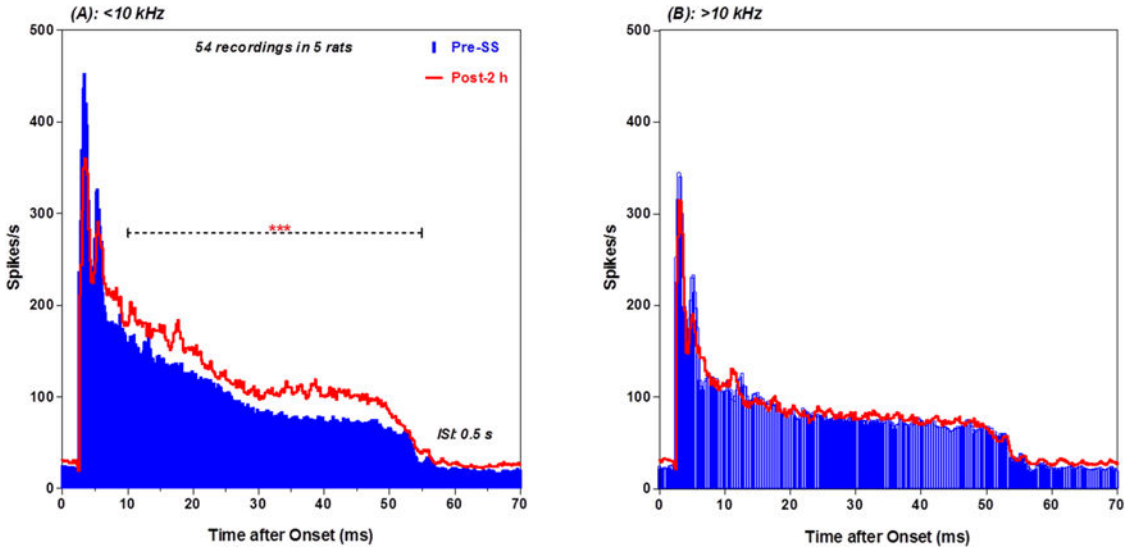

Figure 10.

SS altered low frequency PnC PSTH: (A) Mean (n = 54 MUC from 5 rats) PSTH evoked by 100 dB SPL tone bursts (1–8 kHz, 50 ms, 0.5 s ISI) pre-(blue) and post-SS (red). Discharge rate in the late segment increased significantly after SS treatment. (B) Same as in panel A except tone burst stimuli were 12.1–27.7 kHz. PSTH post-SS (red) nearly identical to pre-SS (blue).

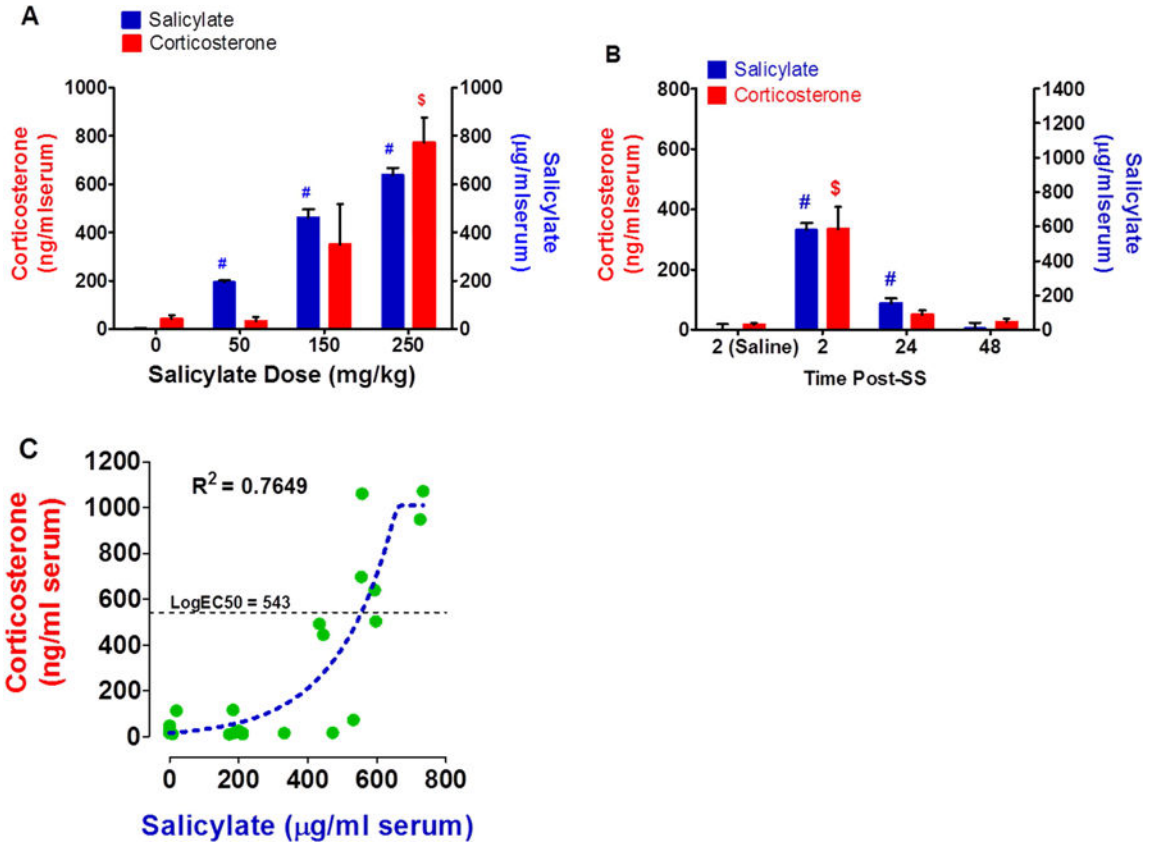

Figure 11.

SS increases serum corticosterone. (A) Histogram showing mean (n = 4) serum salicylate concentration (right ordinate) and mean (n = 4) serum corticosterone concentration (left ordinate) 2 h after intraperitoneal injection of different doses of SS (mg/kg). Serum salicylate concentrations increased with doses; serum salicylate concentrations from 50 to 250 mg/kg were significantly greater (#, $p < 0.05$) than the control (0 mg/kg). Serum corticosterone concentrations increased after the 150 and 250 mg/kg dose of SS. Serum corticosterone concentration was significantly greater than control at 250 mg/kg dose ($, $p < 0.05$). (B) Histogram showing mean (n = 8) serum salicylate concentration (right ordinate) and mean (n = 4) serum corticosterone concentration pre-SS (saline control) and 2, 4 or 48 h after intraperitoneal injection of 250 mg/kg SS. Serum salicylate concentrations were significantly greater than control at 2 and 24 h post-SS (#, $p < 0.05$). Serum corticosterone concentration was significantly greater than the control at 2 h post-SS ($, $p < 0.05$). (C) Scatterplot showing the relationship between serum salicylate concentration and serum corticosterone concentration for different intraperitoneal doses of SS. Dashed line sigmoidal function fit to the data (r2 = 0.7649, Log EC50 = 543.4 mg/ml corticosterone).